FOI
SWEDISH DEFENCE
RESEARCH AGENCY

April 2001
ISSN 1650-1942

Scientific Report

Rikard Gustafsson and Jan Nordström

High Order Finite Difference Approximations of Electromagnetic Wave Propagation Close to Material Discontinuities

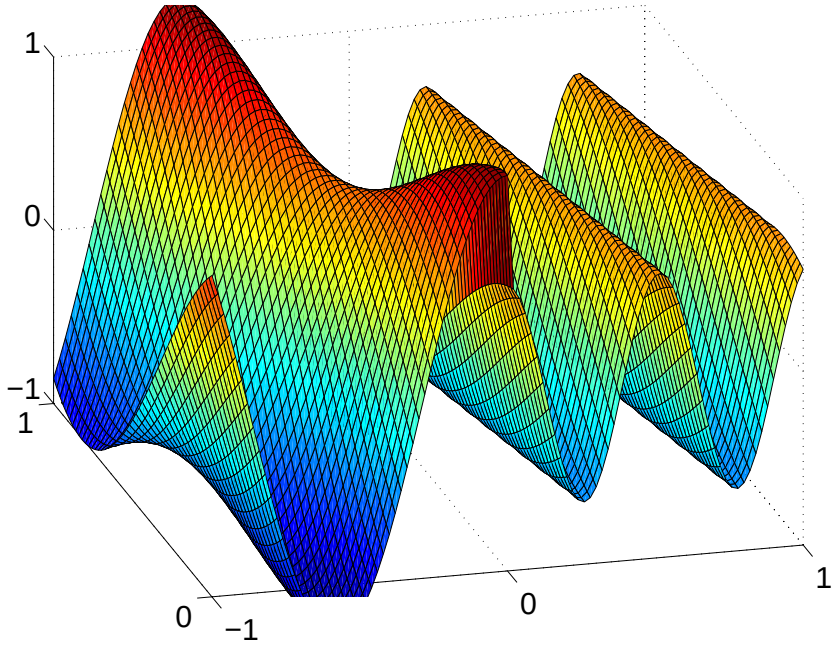

Division of Aeronautics, FFA
SE-172 90 STOCKHOLM

Division of Aeronautics, FFA
SE-172 90 STOCKHOLM

April 2001
ISSN 1650-1942

Scientific Report

Rikard Gustafsson and Jan Nordström

High Order Finite Difference Approximations of Electromagnetic Wave Propagation Close to Material Discontinuities

Division of Aeronautics, FFA
SE-172 90 STOCKHOLM

Abstract

In this paper, electromagnetic wave propagation close to a material discontinuity have been simulated. We have used summation by part (SBP) operators of second, fourth and sixth order accuracy. The boundary conditions have been imposed by the simultaneous approximation term (SAT) procedure. Stability has been shown and the order of accuracy have been verified numerically.

Contents

1 Introduction

When developing a modern fighter aircraft, not only the flying properties but also the visibility of the aircraft is important. The radar equipment sends out electromagnetic waves which propagate towards the aircraft, where it is reflected back to the radar equipment that detects the aircraft. To make the aircraft less visible to radar, these reflections must be minimized.

One approach to minimize radar reflections is to introduce one or several layers of absorbing materials at the surface of the aircraft. In this report we simulate how an electromagnetic wave behaves close to such material discontinuities.

The approximation of Maxwell's equations, which describes electromagnetic wave propagation, is done by using finite difference operators that satisfy a summation by parts (SBP) rule. We will use SBP operators of second, fourth and sixth order accuracy in space and the classical fourth order Runge-Kutta in time.

2 The physics

To describe the physics of electromagnetic fields we have the Maxwell equations

$$\nabla \cdot \boldsymbol{E} = \frac{\rho}{\epsilon}, \tag{1}$$

$$\nabla \times \boldsymbol{E} = -\mu \frac{\partial \boldsymbol{H}}{\partial t}, \tag{2}$$

$$\nabla \cdot \mu \boldsymbol{H} = 0, \tag{3}$$

$$\nabla \times \boldsymbol{H} = \boldsymbol{J} + \epsilon \frac{\partial \boldsymbol{E}}{\partial t}, \tag{4}$$

and the equation of continuity

$$\frac{\partial \rho}{\partial t} + \nabla \cdot \boldsymbol{J} = 0. \tag{5}$$

Here $\boldsymbol{E}$ is the electric field, $\boldsymbol{H}$ the magnetic field, $\boldsymbol{J}$ is the electric current density and ρ is the charge density. ϵ and μ are permittivity and permeability respectively. ϵ and μ can be written as $\epsilon = \epsilon_r \epsilon_0$ and $\mu = \mu_r \mu_0$. ϵ_0 is the permittivity in free space (a material independent constant) and ϵ_r is the relative permittivity (a dimensionless constant which describe the electrical properties of the material). The same goes for μ which describes the magnetic properties.

Our goal is to compute a solution in a domain with a material discontinuity. In particular we need to know what interface conditions will represent the physics of the fields close to the discontinuity.

2.1 The divergence and the normal components

Let us consider a general vector field $\boldsymbol{F}(\boldsymbol{r})$. We can write its source equations in the form

$$\nabla \cdot \boldsymbol{F} = b(\boldsymbol{r}) \quad and \quad \nabla \times \boldsymbol{F} = \boldsymbol{c}(\boldsymbol{r}). \tag{6}$$

Gauss divergence theorem combined with eq.(6) yields

Figure 1. Cylinder used to find boundary condition from Gauss divergence theorem.

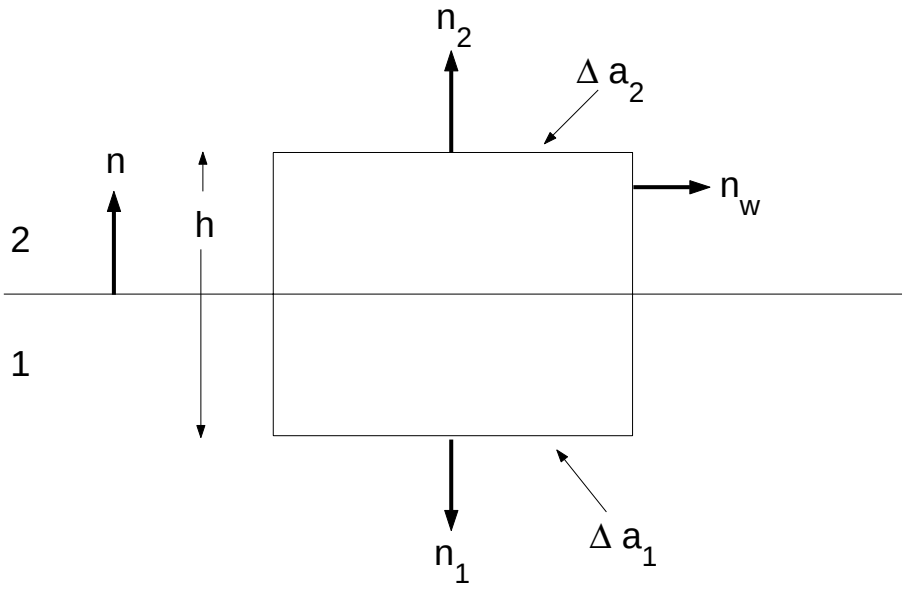

$$\oint_S \boldsymbol{F} \cdot d\boldsymbol{a} = \int_V \nabla \cdot \boldsymbol{F} d\tau = \int_V b(\boldsymbol{r}) d\tau. \tag{7}$$

We apply this to a small cylinder of height h and cross-section area Δa placed over the surface of discontinuity as shown in figure 1. This is done to get a contribution from both region 1 and 2. We choose the area Δa to be small enough so it will be a good approximation to take $\boldsymbol{F}$ to be constant over these faces. The surface integral in eq.(7) can then be written as.

$$\oint_S \boldsymbol{F} \cdot d\boldsymbol{a} = \boldsymbol{F}_2 \cdot \Delta \boldsymbol{a}_2 + \boldsymbol{F}_1 \cdot \Delta \boldsymbol{a}_1 + W, \tag{8}$$

where $\boldsymbol{F}_2$ and $\boldsymbol{F}_1$ are the values on the faces in respective region and W is the contribution from the curved wall of the cylinder. We see from figure 1 that $\boldsymbol{n}_2 = \boldsymbol{n}$ and $\boldsymbol{n}_1 = -\boldsymbol{n}$ so that we can write eq.(8) as

$$\boldsymbol{n} \cdot (\boldsymbol{F}_2 - \boldsymbol{F}_1)\Delta a + W = \int_V b d\tau = (hb)\Delta a, \tag{9}$$

where again Δa is so small that we can take b to be approximately constant.

Now let us shrink the height of the cylinder by letting $h \to 0$ while we keep Δa constant. Since W is proportional to h, $W \to 0$ as $h \to 0$. However b might increase in such a way that $lim_{h\to 0}(hb)$ survives. Since $\boldsymbol{n} \cdot \boldsymbol{F} = F_n$ is the normal component of $\boldsymbol{F}$, we have the final expression for the normal component through a surface of discontinuity.

$$\boldsymbol{F}_{2n} - \boldsymbol{F}_{1n} = \lim_{h\to 0}(hb) = \lim_{h\to 0}(h\nabla \cdot \boldsymbol{F}). \tag{10}$$

If this difference is nonzero, we have a discontinuity in the normal component of the vector field $\boldsymbol{F}$.

2.2 The curl and the tangential components

Stokes´ theorem combined with eq.(6) yields

$$\oint_C \boldsymbol{F} \cdot d\boldsymbol{s} = \int_S (\nabla \times \boldsymbol{F}) \cdot d\boldsymbol{a} = \int_S \boldsymbol{c}(\boldsymbol{r}) \cdot d\boldsymbol{a}. \tag{11}$$

We apply this to a small rectangular path placed perpendicular to the surface of discontinuity as shown in figure 2, so that the sides of length Δs will give us contributions from both regions. The path of integration C is taken counter clockwise, $\boldsymbol{t}_1$ and $\boldsymbol{t}_2$ are unit vectors in their directions respectively and are parallel to the surface of discontinuity. The vector $\boldsymbol{n'}$ is the normal to the area enclosed by the path C and is parallel to the surface between region 1 and 2, thus $\boldsymbol{n'}$ is perpendicular to $\boldsymbol{n}$, the normal to the surface of discontinuity. We also define a vector $\boldsymbol{t}$ so that $\boldsymbol{t}_1 = -\boldsymbol{t}$ and $\boldsymbol{t}_2 = \boldsymbol{t}$. The vectors, $\boldsymbol{n}$, $\boldsymbol{t}$ and q$\boldsymbol{n'}$ are a set of mutually perpendicular unit vectors and satisfy the following properties

Figure 2. Area used to find boundary condition from Stokes' theorem.

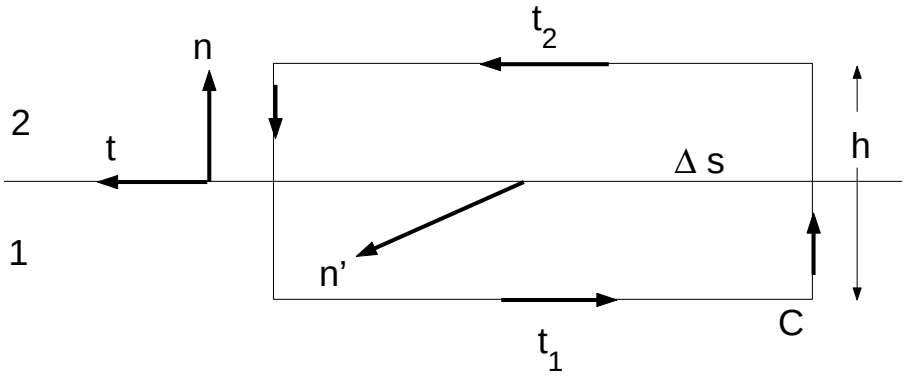

$$\boldsymbol{n'} = \boldsymbol{n} \times \boldsymbol{t} \quad \boldsymbol{t} = \boldsymbol{n'} \times \boldsymbol{n} \quad \boldsymbol{n} = \boldsymbol{t} \times \boldsymbol{n'}. \tag{12}$$

The vector area of this rectangle is $d\boldsymbol{a} = \boldsymbol{n'} h \Delta s$. Eq.(11),(12) leads to

$$\begin{aligned}\oint_C \boldsymbol{F}\cdot d\boldsymbol{s} &= \boldsymbol{F}_1\cdot\boldsymbol{t}_1\Delta s+\boldsymbol{F}_2\cdot\boldsymbol{t}_2\Delta s+\mathcal{W}\\ &= \boldsymbol{t}\cdot(\boldsymbol{F}_2-\boldsymbol{F}_1)\Delta s+\mathcal{W}=\boldsymbol{c}\cdot\boldsymbol{n}'h\Delta s,\end{aligned} \tag{13}$$

where $\boldsymbol{F}_1$, $\boldsymbol{F}_2$ are the values of $\boldsymbol{F}$ in region 1 and 2 respectively, $\mathcal{W}$ is the contribution to the line integral from the ends of the path. Again $\Delta\boldsymbol{s}$ and $h\Delta\boldsymbol{s}$ are so small that a good approximation is to take $\boldsymbol{F}_1$ and $\boldsymbol{F}_2$ to be constant in the area. Now we again let $h\to 0$ while we keep $\Delta\boldsymbol{s}$ constant. $\mathcal{W}$ is proportional to h and will therefore vanish. With use of eq.(12) we write eq.(13) as

$$\boldsymbol{n}'\cdot\left[\boldsymbol{n}\times(\boldsymbol{F}_2-\boldsymbol{F}_1)-\lim_{h\to 0}(h\boldsymbol{c})\right]=0. \tag{14}$$

The orientation of the path of integration is arbitrary, so $\boldsymbol{n}'$ can correspond to an arbitrary direction in the surface. The only way to make sure that eq.(14) is satisfied is to let

$$\boldsymbol{n}\times(\boldsymbol{F}_2-\boldsymbol{F}_1)=\lim_{h\to 0}(h\boldsymbol{c})=\lim_{h\to 0}\left[h(\nabla\times\boldsymbol{F})\right]. \tag{15}$$

If we now cross both sides with $\boldsymbol{n}$ from the right, and use vector analysis, we get

$$\boldsymbol{F}_{2t}-\boldsymbol{F}_{1t}=\lim_{h\to 0}\left[h(\boldsymbol{c}\times\boldsymbol{n})\right]=\lim_{h\to 0}\left\{h\left[(\nabla\times\boldsymbol{F})\times\boldsymbol{n}\right]\right\}. \tag{16}$$

If the righthand side of eq.(16) is nonzero, we have a discontinuity in the tangential component of $\boldsymbol{F}$

We have now obtained a way of finding how the vector $\boldsymbol{F}$ changes as we go across a surface of discontinuity. Suppose we know $\boldsymbol{F}_1$ we then split it into its normal and tangential components $\boldsymbol{F}_{1n}$ and $\boldsymbol{F}_{1t}$. We then get the normal component of $\boldsymbol{F}_2$ from eq.(10), and its tangential component from eq.(16). By combining these components we get $\boldsymbol{F}_2$.

2.3 Interface condition for the electric field

Let $\boldsymbol{F}$ be the electric field $\boldsymbol{E}$, eq.(2) and eq.(16) leads to

$$\boldsymbol{E}_{2t}-\boldsymbol{E}_{1t}=\lim_{h\to 0}\left\{h\left[\left(-\mu\frac{\partial\boldsymbol{H}}{\partial t}\right)\times\boldsymbol{n}\right]\right\}. \tag{17}$$

As we let $h\to 0$ we expect that $\frac{\partial\boldsymbol{H}}{\partial t}$ will remain finite. This means that the tangential components of $\boldsymbol{E}$ are continuous over a surface of discontinuity, i.e.

$$\boldsymbol{E}_{2t} - \boldsymbol{E}_{1t} = 0. \tag{18}$$

Now follow the procedure in section 2.1 and let $\boldsymbol{F}$ be the electric field $\boldsymbol{E}$. eq.(1) and eq.(7) leads to

$$\oint_S \boldsymbol{E} \cdot d\boldsymbol{a} = \frac{1}{\epsilon} \int_V \rho d\tau = \frac{\rho h \Delta a}{\epsilon} = \frac{\Delta q}{\epsilon}, \tag{19}$$

where Δq is the total charge inside the volume $h\Delta a$. As we let $h \to 0$, the total charge Δq must be conserved. In the limit, the charge is described as a *surface charge* of density σ. Therefore we get

$$\Delta q = \sigma \Delta a = \left(\lim_{h \to 0} h\rho \right) \Delta a, \quad \sigma = \lim_{h \to 0} (h\rho). \tag{20}$$

Eq.(10) now gives us the interface condition for the normal component

$$\boldsymbol{E}_{2n} - \boldsymbol{E}_{1n} = \lim_{h \to 0} (h \nabla \cdot \boldsymbol{E}) = \lim_{h \to 0} \left(h \frac{\rho}{\epsilon} \right) = \frac{\sigma}{\epsilon}. \tag{21}$$

There will be a discontinuity in the normal component of $\boldsymbol{E}$ only if there is a surface charge on the surface separating the two regions. However charges can be divided in two classes, *bound charges* ρ_b and *free charges* ρ_f, and it is only the free charges we can control. The bound charges depends of the material. We have

$$\rho = \rho_f + \rho_b = \rho_f - \nabla \cdot \boldsymbol{P} \tag{22}$$

where $\boldsymbol{P}$ is the *polarization*. When this is substituted into eq(1), we get

$$\nabla \cdot (\epsilon_0 \boldsymbol{E} + \boldsymbol{P}) = \rho_f. \tag{23}$$

And we define a vector, $\boldsymbol{D} = \epsilon_0 \boldsymbol{E} + \boldsymbol{P}$, called the *electric displacement*. In linear isotropic dielectrics we can write $\boldsymbol{D} = \epsilon_r \epsilon_0 \boldsymbol{E}$. Now let $\boldsymbol{F}$ be the electric displacement vector $\boldsymbol{D}$. We get the interface conditions from eq.(10) and (20)

$$\boldsymbol{D}_{2n} - \boldsymbol{D}_{1n} = \epsilon_2 \epsilon_0 \boldsymbol{E}_{2n} - \epsilon_1 \epsilon_0 \boldsymbol{E}_{1n} = \sigma_f. \tag{24}$$

The interface condition for the normal component of $\boldsymbol{E}$ becomes

$$\epsilon_2 \boldsymbol{E}_{2n} - \epsilon_1 \boldsymbol{E}_{1n} = \tfrac{\sigma_f}{\epsilon_0}, \quad \text{or} \quad \boldsymbol{E}_{2n} = \tfrac{1}{\epsilon_2} \left(\epsilon_1 \boldsymbol{E}_{1n} + \tfrac{\sigma_f}{\epsilon_0} \right). \tag{25}$$

If there are no free charges at the interface there is a discontinuity in the normal component of $\boldsymbol{E}$ only if the two regions represent materials of different electric properties.

2.4 Interface conditions for the magnetic field

Let $\boldsymbol{F}$ be the magnetic field $\boldsymbol{H}$, eq.(4) and eq.(16) leads to

$$\boldsymbol{H}_{2t} - \boldsymbol{H}_{1t} = \lim_{h\to 0}\left\{ h\left[\left(\boldsymbol{J}_f + \epsilon\frac{\partial \boldsymbol{E}}{\partial t}\right)\times \boldsymbol{n}\right]\right\}. \tag{26}$$

As we let $h \to 0$ we expect that $\frac{\partial \boldsymbol{E}}{\partial t}$ will remain finite. In the limit, the current density $\boldsymbol{J}_f$ is described as a *surface current* of density $\boldsymbol{K}$. Therefore we get

$$\boldsymbol{H}_{2t} - \boldsymbol{H}_{1t} = \lim_{h\to 0}\left[h(\boldsymbol{J}_f \times \boldsymbol{n})\right] = \boldsymbol{K}. \tag{27}$$

There is a discontinuity in the tangential component of $\boldsymbol{H}$ only if there is a surface current density at the interface.

To find the interface condition for the normal component of $\boldsymbol{H}$, let $\boldsymbol{F}$ in eq.(10) be the magnetic field $\boldsymbol{H}$, according to eq.(3), the interface condition for the normal component becomes

$$\mu_2\mu_0\boldsymbol{H}_{2n} - \mu_1\mu_0\boldsymbol{H}_{1n} = 0, \quad \text{or} \quad \boldsymbol{H}_{2n} = \tfrac{\mu_1}{\mu_2}\boldsymbol{H}_{1n}. \tag{28}$$

The normal component of the magnetic field $\boldsymbol{H}$ will be discontinuous over the interface only if the two regions represent materials of different magnetic properties.

3 The continuous problem

In a lossless medium we can write the 2D maxwell equation in TE (transverse electric) mode as

$$\begin{cases} \boldsymbol{S}_l \boldsymbol{u}_t + \boldsymbol{F}_{xl} + \boldsymbol{G}_{yl} = 0 \\ \boldsymbol{S}_r \boldsymbol{v}_t + \boldsymbol{F}_{xr} + \boldsymbol{G}_{yr} = 0, \end{cases} \tag{29}$$

where $\boldsymbol{F}_l = \boldsymbol{A}\boldsymbol{u}$, $\boldsymbol{G}_l = \boldsymbol{B}\boldsymbol{u}$, $\boldsymbol{F}_r = \boldsymbol{A}\boldsymbol{v}$, $\boldsymbol{G}_r = \boldsymbol{B}\boldsymbol{v}$ and

$$\boldsymbol{A} = \begin{pmatrix} 0 & 0 & 1 \\ 0 & 0 & 0 \\ 1 & 0 & 0 \end{pmatrix}, \quad \boldsymbol{B} = \begin{pmatrix} 0 & -1 & 0 \\ -1 & 0 & 0 \\ 0 & 0 & 0 \end{pmatrix}, \quad \boldsymbol{S}_l = \begin{pmatrix} \mu_l & 0 & 0 \\ 0 & \epsilon_l & 0 \\ 0 & 0 & \epsilon_l \end{pmatrix},$$

$$\boldsymbol{u} = \begin{pmatrix} \boldsymbol{H}_{zl} \\ \boldsymbol{E}_{xl} \\ \boldsymbol{E}_{yl} \end{pmatrix}, \qquad \boldsymbol{v} = \begin{pmatrix} \boldsymbol{H}_{zr} \\ \boldsymbol{E}_{xr} \\ \boldsymbol{E}_{yr} \end{pmatrix}, \qquad \boldsymbol{S}_r = \begin{pmatrix} \mu_r & 0 & 0 \\ 0 & \epsilon_r & 0 \\ 0 & 0 & \epsilon_r \end{pmatrix}.$$

Also, the conditions at the material discontinuity are (see section 2)

$$\boldsymbol{v}(x=0) = \boldsymbol{\Gamma}\boldsymbol{u}(x=0), \quad \text{where} \quad \boldsymbol{\Gamma} = \begin{pmatrix} 1 & 0 & 0 \\ 0 & \frac{\epsilon_r}{\epsilon_l} & 0 \\ 0 & 0 & 1 \end{pmatrix}. \tag{30}$$

3.1 The continuous interface conditions

Multiply eq.(29) with Φ ,where $\Phi(x, y, t)$ is a continuous test function that vanishes on the outer boundaries and at $t = 0, \infty$. Integrate in time and space and add the equations

$$\begin{aligned} &\int_0^\infty \int_0^1 \int_{-1}^0 \boldsymbol{\Phi}\Big(\boldsymbol{S}_l \boldsymbol{u}_t + \boldsymbol{F}_{xl} + \boldsymbol{G}_{yl}\Big)\, dxdydt \\ &+ \int_0^\infty \int_0^1 \int_0^1 \boldsymbol{\Phi}\Big(\boldsymbol{S}_r \boldsymbol{v}_t + \boldsymbol{F}_{xr} + \boldsymbol{G}_{yr}\Big)\, dxdydt = 0. \end{aligned} \tag{31}$$

By making use of the fact that Φ is continuous over the interface and vanishes at the outer boundaries and at $t = 0, \infty$, we get

Figure 3. The computational domain.

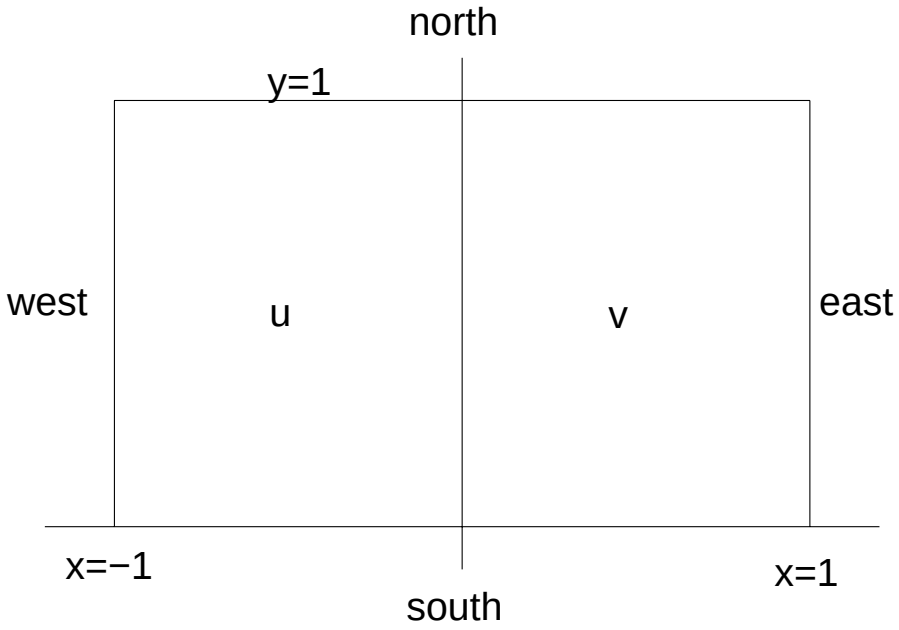

$$\int_0^\infty \int_0^1 \int_{-1}^0 \Big(\boldsymbol{\Phi}_t \boldsymbol{S}_l \boldsymbol{u} + \boldsymbol{\Phi}_x \boldsymbol{F}_l + \boldsymbol{\Phi}_y \boldsymbol{G}_l \Big) dxdydt$$
$$+ \int_0^\infty \int_0^1 \int_0^1 \Big(\boldsymbol{\Phi}_t \boldsymbol{S}_r \boldsymbol{v} + \boldsymbol{\Phi}_x \boldsymbol{F}_r + \boldsymbol{\Phi}_y \boldsymbol{G}_r \Big) dxdydt \qquad (32)$$
$$+ \int_0^\infty \int_0^1 \boldsymbol{\Phi} \Big(\boldsymbol{F}_r(x=0) - \boldsymbol{F}_l(x=0) \Big) dydt = 0.$$

$\boldsymbol{F}_l = \boldsymbol{A}\boldsymbol{u}, \boldsymbol{F}_r = \boldsymbol{A}\boldsymbol{v}$ and the interface condition $\boldsymbol{u}(x=0) = \boldsymbol{\Gamma}\boldsymbol{v}(x=0)$ removes the interface terms.

3.2 The continuous energy estimate

If we define a new vector $\boldsymbol{W} = (\boldsymbol{u}, \boldsymbol{v})^T$, set $\boldsymbol{F} = diag(\boldsymbol{A}, \boldsymbol{A})\boldsymbol{W}$ and $\boldsymbol{G} = diag(\boldsymbol{B}, \boldsymbol{B})\boldsymbol{W}$, $\boldsymbol{S} = diag(\boldsymbol{S}_l, \boldsymbol{S}_r)$, we can write eq.(29) as

$$\boldsymbol{S}\boldsymbol{W}_t + \boldsymbol{F}_x + \boldsymbol{G}_y = 0. \qquad (33)$$

Multiplication of eq. (33) with $\boldsymbol{W}^T$, integration in space and the fact that the matrices $\boldsymbol{A}$ and $\boldsymbol{B}$ are symmetric, leads to

$$
\begin{aligned}
\frac{d}{dt}\|\boldsymbol{W}\|_S^2 &= \int_0^1\int_{-1}^1 \boldsymbol{W}^T\boldsymbol{S}\boldsymbol{W}_t dxdy \\
&= -\int_0^1 \boldsymbol{W}^T\boldsymbol{F}|_{x=-1}^{x=1} dy - \int_{-1}^1 \boldsymbol{W}^T\boldsymbol{G}|_{y=0}^{y=1} dx \\
&= -\int_0^1 \left(\boldsymbol{u}^T\boldsymbol{A}\boldsymbol{u}|_{x=-1}^{x=0} + \boldsymbol{v}^T\boldsymbol{A}\boldsymbol{v}|_{x=0}^{x=1}\right) dy \\
&\quad -\int_{-1}^0 \boldsymbol{u}^T\boldsymbol{B}\boldsymbol{u}|_{y=0}^{y=1} dx - \int_0^1 \boldsymbol{v}^T\boldsymbol{B}\boldsymbol{v}|_{y=0}^{y=1} dx.
\end{aligned}
\tag{34}
$$

After evaluation we get

$$
\begin{aligned}
\frac{d}{dt}\|\boldsymbol{W}\|_S^2 = &\underbrace{-2\int_0^1 H_z E_y|_{x=1} dy}_{east} + \underbrace{2\int_0^1 H_z E_y|_{x=-1} dy}_{west} \\
&\underbrace{+2\int_{-1}^0 H_z E_x|_{y=1} dx + 2\int_0^1 H_z E_x|_{y=1} dx}_{north} \\
&\underbrace{-2\int_{-1}^0 H_z E_x|_{y=0} dx - 2\int_0^1 H_z E_x|_{y=0} dx}_{south}.
\end{aligned}
\tag{35}
$$

The method is well-posed if we specify the E_y component at the west and east boundary and the E_x component at the south and north boundary. Note: by specifying the ingoing characteristics we can obtain a strongly well-posed method, see [1].

3.3 The divergence of $\boldsymbol{E}$ and $\boldsymbol{H}$

Consider the continuous problem, away from the interface. The divergence of eq.(4) and eq.(5) leads to

$$
\frac{\partial}{\partial t}\left(\epsilon\nabla\cdot\boldsymbol{E} - \rho\right) = 0, \tag{36}
$$

and we have

$$
\left(\nabla\cdot\boldsymbol{E} - \frac{\rho}{\epsilon}\right)(t) = \left(\nabla\cdot\boldsymbol{E} - \frac{\rho}{\epsilon}\right)(0). \tag{37}
$$

This means that if $\nabla \cdot \boldsymbol{E} - \frac{\rho}{\epsilon} = 0$ initially, eq.(1) will be satisfied for all t. The divergence of eq.(2) leads to

$$(\nabla \cdot \mu \boldsymbol{H})(t) = (\nabla \cdot \mu \boldsymbol{H})(0), \tag{38}$$

hence if $\nabla \cdot \boldsymbol{H} = 0$ initially, eq.(3) will be satisfied for all t. This shows that eq.(1) and (3) follows from eq.(2), (4) and (5).

4 The discrete problem

The spatial discretization is made by introducing a 2D grid, see figure 4, with node points (x_i, y_j), where $i = 0, 1, \ldots, N$ and $j = 0, 1, \ldots, M$. The unknowns are organized in a vector $\boldsymbol{u}$ with the following enumeration

$$\boldsymbol{u} = \begin{pmatrix} \boldsymbol{u}_0(t) \\ \boldsymbol{u}_1(t) \\ \vdots \\ \boldsymbol{u}_N(t) \end{pmatrix}, \quad \boldsymbol{u}_i(t) = \begin{pmatrix} \boldsymbol{u}_{i,0}(t) \\ \boldsymbol{u}_{i,1}(t) \\ \vdots \\ \boldsymbol{u}_{i,M}(t) \end{pmatrix}, \quad \boldsymbol{u}_{i,j} = \begin{pmatrix} H_z \\ E_x \\ E_y \end{pmatrix}. \tag{39}$$

The vector $\boldsymbol{u}_{i,j}$ corresponds to the grid point (x_i, y_j). At the interface $x = 0$, $\boldsymbol{u}_N$ and $\boldsymbol{v}_0$ correspond to the same grid points. To simplify the notation we also introduce an alternative enumeration of the unknowns

$$\hat{\boldsymbol{u}}_j(t) = \begin{pmatrix} \boldsymbol{u}_{0,j}(t) \\ \boldsymbol{u}_{1,j}(t) \\ \vdots \\ \boldsymbol{u}_{N,j}(t) \end{pmatrix}, \quad j = 0, 1, \ldots, M. \tag{40}$$

Figure 4. The 2D grid.

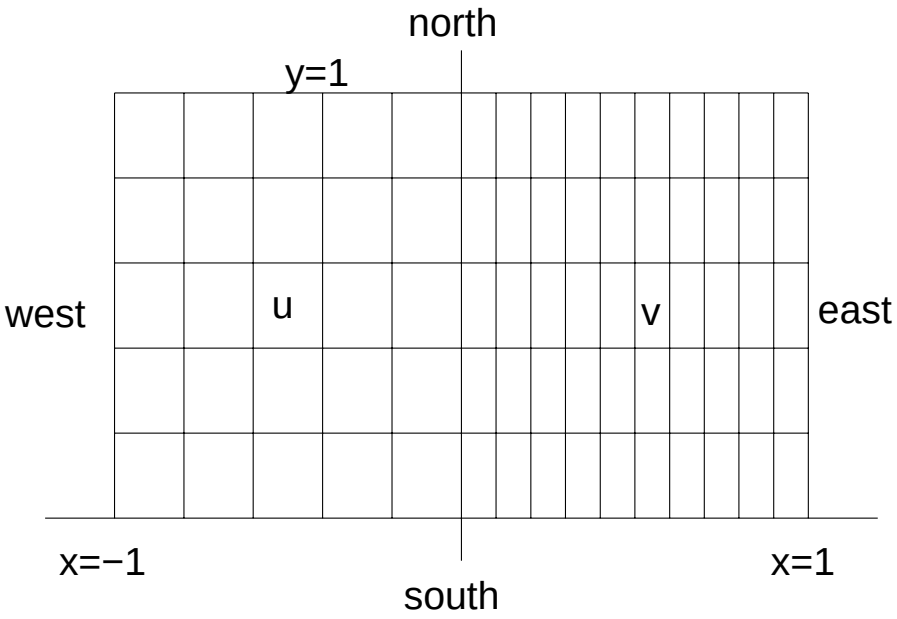

We will use SBP (Summation By Parts) operators, for the spatial discretization. The SBP method [2] is a way of constructing an operator for discretization of the numerical first derivative. The spatial operator is introduced as

$$u_x = P^{-1}Qu, \tag{41}$$

where P and Q are matrices. If a spatial operator is of the form (41) and the conditions (i) and (ii) below are full-filled the operator is referred to as a Summation By Parts operator.

(i) The matrix P is symmetric, positive definite and bounded, $\Delta xpI \leq P \leq \Delta xqI$, where $p > 0$ and q are bounded independent of N.

(ii) The matrix Q is almost skew-symmetric. $Q+Q^T = diag(-1, 0, \ldots, 0, 1)$.

The boundary conditions will be imposed by the SAT (Simultaneous Approximation Term) procedure, [4]. The semi-discrete equation for the two domain problem becomes

$$\begin{cases} \boldsymbol{S}_l \boldsymbol{u}_t + \Big(\boldsymbol{P}_{xl}^{-1}\boldsymbol{Q}_{xl} \otimes \boldsymbol{I}_M \otimes \boldsymbol{A}\Big)\boldsymbol{u} + \Big(\boldsymbol{I}_{Nl} \otimes \boldsymbol{P}_y^{-1}\boldsymbol{Q}_y \otimes \boldsymbol{B}\Big)\boldsymbol{u} = \boldsymbol{BC}_l \\ \quad + \Big(\boldsymbol{P}_{xl}^{-1}\boldsymbol{E}_{NlNl} \otimes \boldsymbol{I}_M \otimes \boldsymbol{\Sigma}_{x=0l}\Big)\Big(\boldsymbol{u} - \boldsymbol{e}_{NlNl} \otimes \big((\boldsymbol{I}_M \otimes \Gamma)\boldsymbol{v}_0\big)\Big) \\ \boldsymbol{S}_r \boldsymbol{v}_t + \Big(\boldsymbol{P}_{xr}^{-1}\boldsymbol{Q}_{xr} \otimes \boldsymbol{I}_M \otimes \boldsymbol{A}\Big)\boldsymbol{v} + \Big(\boldsymbol{I}_{Nr} \otimes \boldsymbol{P}_y^{-1}\boldsymbol{Q}_y \otimes \boldsymbol{B}\Big)\boldsymbol{v} = \boldsymbol{BC}_r \\ \quad + \Big(\boldsymbol{P}_{xr}^{-1}\boldsymbol{E}_{0Nr} \otimes \boldsymbol{I}_M \otimes \boldsymbol{\Sigma}_{x=0r}\Big)\Big(\boldsymbol{v} - \boldsymbol{e}_{0Nr} \otimes \big((\boldsymbol{I}_M \otimes \Gamma^{-1})\boldsymbol{u}_{Nl}\big)\Big). \end{cases} \tag{42}$$

Here $\boldsymbol{I}_L$ are identity matrices of size $(L+1)\times(L+1)$, $\boldsymbol{E}_{LL}$ and $\boldsymbol{E}_{0L}$ are matrices of size $(L+1)\times(L+1)$, where L can be Nl, Nr or M.

$$\boldsymbol{E}_{0L} = \begin{pmatrix} 1 & 0 & \cdots & 0 \\ 0 & 0 & & \\ \vdots & & \ddots & \\ 0 & & & 0 \end{pmatrix}, \quad \boldsymbol{E}_{LL} = \begin{pmatrix} 0 & 0 & \cdots & 0 \\ 0 & 0 & & \\ \vdots & & \ddots & \\ 0 & & & 1 \end{pmatrix}, \tag{43}$$

and $\boldsymbol{e}_{0L}$ and $\boldsymbol{e}_{LL}$ are vectors of length $L+1$

$$\boldsymbol{e}_{0L} = \begin{pmatrix} 1 & 0 & \cdots & 0 \end{pmatrix}^T, \quad \boldsymbol{e}_{LL} = \begin{pmatrix} 0 & 0 & \cdots & 1 \end{pmatrix}^T. \tag{44}$$

$\boldsymbol{BC}_l$ and $\boldsymbol{BC}_r$ are the penalty terms including boundary conditions im-

posed by the SAT method.

$$
\begin{aligned}
\boldsymbol{BC}_l = & \underbrace{(\boldsymbol{P}_x^{-1}\boldsymbol{E}_{0Nl} \otimes \boldsymbol{I}_M \otimes \boldsymbol{\Sigma}_{x=-1})(\boldsymbol{u} - \boldsymbol{e}_{0Nl} \otimes \boldsymbol{g}_1)}_{west} \\
& + \underbrace{(\boldsymbol{I}_{Nl} \otimes \boldsymbol{P}_y^{-1}\boldsymbol{E}_{0M} \otimes \boldsymbol{\Sigma}_{y=0})(\boldsymbol{u} - \boldsymbol{g}_{2l} \otimes \boldsymbol{e}_{0M})}_{south} \\
& + \underbrace{(\boldsymbol{I}_{Nl} \otimes \boldsymbol{P}_y^{-1}\boldsymbol{E}_{MM} \otimes \boldsymbol{\Sigma}_{y=1})(\boldsymbol{u} - \boldsymbol{g}_{3l} \otimes \boldsymbol{e}_{MM})}_{north} \\
\boldsymbol{BC}_r = & \underbrace{(\boldsymbol{P}_x^{-1}\boldsymbol{E}_{NrNr} \otimes \boldsymbol{I}_M \otimes \boldsymbol{\Sigma}_{x=1})(\boldsymbol{v} - \boldsymbol{e}_{NrNr} \otimes \boldsymbol{g}_4)}_{east} \\
& + \underbrace{(\boldsymbol{I}_{Nr} \otimes \boldsymbol{P}_y^{-1}\boldsymbol{E}_{0M} \otimes \boldsymbol{\Sigma}_{y=0})(\boldsymbol{v} - \boldsymbol{g}_{2r} \otimes \boldsymbol{e}_{0M})}_{south} \\
& + \underbrace{(\boldsymbol{I}_{Nr} \otimes \boldsymbol{P}_y^{-1}\boldsymbol{E}_{MM} \otimes \boldsymbol{\Sigma}_{y=1})(\boldsymbol{v} - \boldsymbol{g}_{3r} \otimes \boldsymbol{e}_{MM})}_{north}
\end{aligned}
\tag{45}
$$

Here $\boldsymbol{E}_{i,j}$ and $\boldsymbol{e}_{i,j}$ are defined as in eq.(43) and (44). The boundary conditions are stored in $\boldsymbol{g}_i$.

To visualize how the two regions are connected to each other we can write the system in the form

$$
\boldsymbol{W}_t = \boldsymbol{M}(\boldsymbol{W} + \boldsymbol{G}) \tag{46}
$$

Where $\boldsymbol{G}$ includes the outer boundary data. In the 6th order case, with M=20, Nl=20, Nr=20, the matrix $\boldsymbol{M}$ is depicted in figure 5. The square in the center of the matrix is the $36M \times 36M$ matrix which couples the two regions.

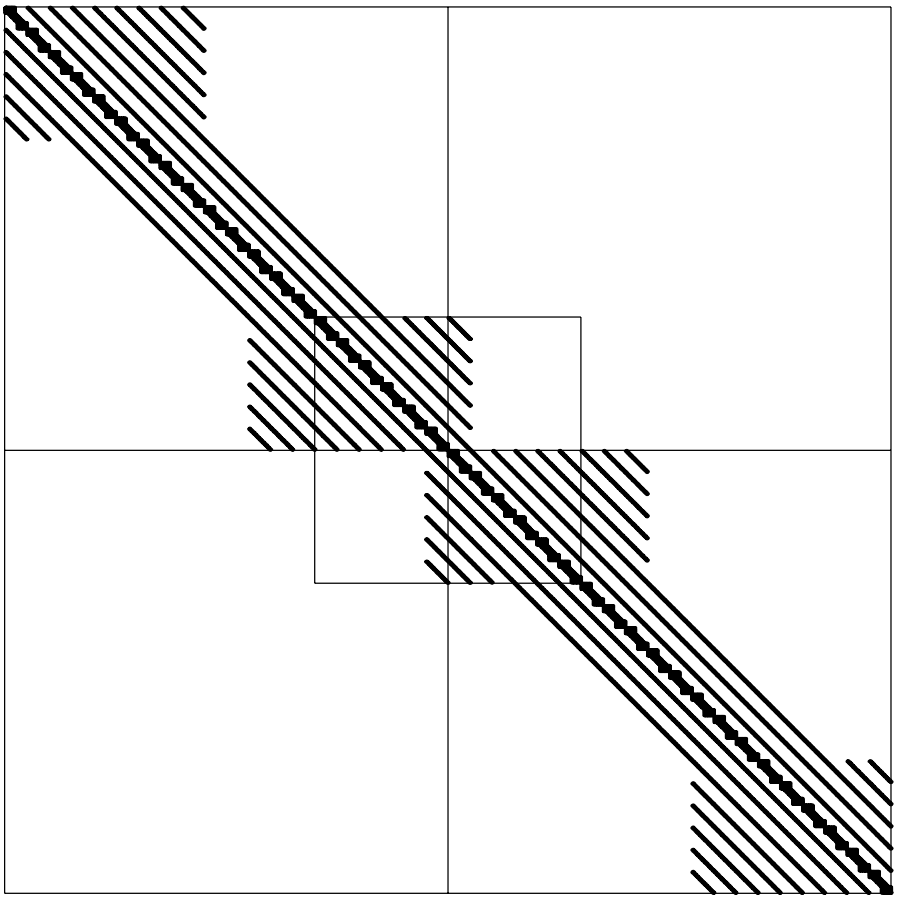

Figure 5. The system matrix in 6th order case with M=20, Nl=20, Nr=20. The $36M \times 36M$ square matrix in the center couples the two regions.

4.1 The numerical interface conditions

Multiply eq.(42) with $\boldsymbol{P}_l = (\boldsymbol{P}_{xl} \otimes \boldsymbol{P}_y \otimes \boldsymbol{I}_3)$ and $\boldsymbol{P}_r = (\boldsymbol{P}_{xr} \otimes \boldsymbol{P}_y \otimes \boldsymbol{I}_3)$ respectively. Let $\boldsymbol{\Phi}(x, y, t)$ be a continuous test function that vanishes on the outer boundaries and at $t = 0, \infty$. We get

$$\begin{cases} \boldsymbol{\Phi}^T \boldsymbol{P}_l \boldsymbol{S}_l \boldsymbol{u}_t + \boldsymbol{\Phi}^T \Big(\boldsymbol{Q}_{xl} \otimes \boldsymbol{P}_y \otimes \boldsymbol{A} \Big) \boldsymbol{u} + \hat{\boldsymbol{\Phi}}^T \Big(\boldsymbol{Q}_y \otimes \boldsymbol{P}_{xl} \otimes \boldsymbol{B} \Big) \hat{\boldsymbol{u}} \\ \qquad = \boldsymbol{\Phi}^T (x = 0) \Big(\boldsymbol{P}_y \otimes \boldsymbol{\Sigma}_{x=0l} \Big) \Big(\boldsymbol{u}_{Nl} - (\boldsymbol{I}_M \otimes \boldsymbol{\Gamma}) \boldsymbol{v}_0) \Big) \\ \boldsymbol{\Phi}^T \boldsymbol{P}_r \boldsymbol{S}_r \boldsymbol{v}_t + \boldsymbol{\Phi}^T \Big(\boldsymbol{Q}_{xr} \otimes \boldsymbol{P}_y \otimes \boldsymbol{A} \Big) \boldsymbol{v} + \hat{\boldsymbol{\Phi}}^T \Big(\boldsymbol{Q}_y \otimes \boldsymbol{P}_{xr} \otimes \boldsymbol{B} \Big) \hat{\boldsymbol{v}} \\ \qquad = \boldsymbol{\Phi}^T (x = 0) \Big(\boldsymbol{P}_y \otimes \boldsymbol{\Sigma}_{x=0r} \Big) \Big(\boldsymbol{v}_0 - (\boldsymbol{I}_M \otimes \boldsymbol{\Gamma}^{-1}) \boldsymbol{u}_{Nl}) \Big). \end{cases} \tag{47}$$

Using the summation by parts properties of $\boldsymbol{Q}_l$ and $\boldsymbol{Q}_r$ in section 4, we get

$$
\begin{cases}
\boldsymbol{\Phi}^T \boldsymbol{P}_l \boldsymbol{S}_l \boldsymbol{u}_t - \boldsymbol{u}^T \Big(\boldsymbol{Q}_{xl} \otimes \boldsymbol{P}_y \otimes \boldsymbol{A} \Big) \boldsymbol{\Phi} - \hat{\boldsymbol{u}}^T \Big(\boldsymbol{Q}_y \otimes \boldsymbol{P}_{xl} \otimes \boldsymbol{B} \Big) \hat{\boldsymbol{\Phi}} \\
\quad = -\boldsymbol{\Phi}^T(x=0) \Big(\boldsymbol{P}_y \otimes \boldsymbol{A} \Big) \boldsymbol{u}_{Nl} \\
\qquad + \boldsymbol{\Phi}^T(x=0) \Big(\boldsymbol{P}_y \otimes \boldsymbol{\Sigma}_{x=0l} \Big) \Big(\boldsymbol{u}_{Nl} - (\boldsymbol{I}_M \otimes \boldsymbol{\Gamma}) \boldsymbol{v}_0 \Big) \\
\boldsymbol{\Phi}^T \boldsymbol{P}_r \boldsymbol{S}_r \boldsymbol{v}_t - \boldsymbol{v}^T \Big(\boldsymbol{Q}_{xr} \otimes \boldsymbol{P}_y \otimes \boldsymbol{A} \Big) \boldsymbol{\Phi} - \hat{\boldsymbol{v}}^T \Big(\boldsymbol{Q}_y \otimes \boldsymbol{P}_{xr} \otimes \boldsymbol{B} \Big) \hat{\boldsymbol{\Phi}} \\
\quad = \boldsymbol{\Phi}^T(x=0) \Big(\boldsymbol{P}_y \otimes \boldsymbol{A} \Big) \boldsymbol{v}_0 \\
\qquad + \boldsymbol{\Phi}^T(x=0) \Big(\boldsymbol{P}_y \otimes \boldsymbol{\Sigma}_{x=0r} \Big) \Big(\boldsymbol{v}_0 - (\boldsymbol{I}_M \otimes \boldsymbol{\Gamma}^{-1}) \boldsymbol{u}_{Nl} \Big).
\end{cases}
\tag{48}
$$

Add the two equations, integrate in time, and make use of the fact that Φ is continuous over the interface, this leads to

$$
\begin{aligned}
&\int_0^\infty \Big(\boldsymbol{\Phi}_t^T \boldsymbol{P}_l \boldsymbol{S}_l \boldsymbol{u} + \boldsymbol{u}^T (\boldsymbol{Q}_{xl} \otimes \boldsymbol{P}_y \otimes \boldsymbol{A}) \boldsymbol{\Phi} + \hat{\boldsymbol{u}}^T (\boldsymbol{Q}_y \otimes \boldsymbol{P}_{xl} \otimes \boldsymbol{B}) \hat{\boldsymbol{\Phi}} \Big) dt \\
+ &\int_0^\infty \Big(\boldsymbol{\Phi}_t^T \boldsymbol{P}_r \boldsymbol{S}_r \boldsymbol{v} + \boldsymbol{v}^T (\boldsymbol{Q}_{xr} \otimes \boldsymbol{P}_y \otimes \boldsymbol{A}) \boldsymbol{\Phi} + \hat{\boldsymbol{v}}^T (\boldsymbol{Q}_y \otimes \boldsymbol{P}_{xr} \otimes \boldsymbol{B}) \hat{\boldsymbol{\Phi}} \Big) dt \\
+ &\int_0^\infty \Phi^T(x=0) \Big(\boldsymbol{P}_y \otimes (\boldsymbol{\Sigma}_{x=0l} - \boldsymbol{\Sigma}_{x=0r} \boldsymbol{\Gamma}^{-1} - \boldsymbol{A}) \Big) \boldsymbol{u}_{Nl} dt \\
+ &\int_0^\infty \Phi^T(x=0) \Big(\boldsymbol{P}_y \otimes (\boldsymbol{\Sigma}_{x=0r} - \boldsymbol{\Sigma}_{x=0l} \boldsymbol{\Gamma} + \boldsymbol{A}) \Big) \boldsymbol{v}_0 dt = 0.
\end{aligned}
\tag{49}
$$

Note the close similarity between eq.(32) and eq.(49). The following condition for $\Sigma_{x=0l}$ and $\Sigma_{x=0r}$ will eliminate the interface terms

$$
\boldsymbol{\Sigma}_{x=0r} = (\boldsymbol{\Sigma}_{x=0l} - \boldsymbol{A}) \boldsymbol{\Gamma} = 0 \tag{50}
$$

To preserve the conservative character of the problem we require condition (50) to be fulfilled.

4.2 The discrete energy estimate

With the use of the so called Q-formulation, see [5], eq. (42) can be written in the following way

$$
\boldsymbol{P} \boldsymbol{W}_t + (\boldsymbol{Q}_x + \boldsymbol{\Sigma}_{int}) \boldsymbol{W} + \boldsymbol{Q}_y \boldsymbol{W} = \boldsymbol{B} \boldsymbol{C}, \tag{51}
$$

where $\boldsymbol{W} = (\boldsymbol{u}, \boldsymbol{v})^T$ and

$$\begin{aligned}
\boldsymbol{P} &= diag\Big((\boldsymbol{P}_{xl} \otimes \boldsymbol{P}_y \otimes \boldsymbol{I}_3)\boldsymbol{S}_l, (\boldsymbol{P}_{xr} \otimes \boldsymbol{P}_y \otimes \boldsymbol{I}_3)\boldsymbol{S}r\Big) \\
\boldsymbol{Q}_x &= diag\Big((\boldsymbol{Q}_{xl} \otimes \boldsymbol{P}_y \otimes \boldsymbol{A}), (\boldsymbol{Q}_{xr} \otimes \boldsymbol{P}_y \otimes \boldsymbol{A})\Big) \\
\boldsymbol{Q}_y &= diag\Big((\boldsymbol{P}_{xl} \otimes \boldsymbol{Q}_y \otimes \boldsymbol{B}), (\boldsymbol{P}_{xr} \otimes \boldsymbol{Q}_y \otimes \boldsymbol{B})\Big).
\end{aligned} \tag{52}$$

$\boldsymbol{BC}$ are the penalty terms including boundary conditions imposed by the SAT procedure

$$\begin{aligned}
\boldsymbol{BC} = &\Big(\boldsymbol{E}_l \otimes \boldsymbol{E}_{0Nl} \otimes \boldsymbol{P}_y \otimes \boldsymbol{\Sigma}_{x=-1}\Big)\Big(\boldsymbol{E}_{\boldsymbol{u}_0}\boldsymbol{W} - \boldsymbol{e}_l \otimes \boldsymbol{e}_{0Nl} \otimes \boldsymbol{g}_1\Big) \\
&+ \Big(\boldsymbol{E}_l \otimes \boldsymbol{E}_{0M} \otimes \boldsymbol{P}_{xl} \otimes \boldsymbol{\Sigma}_{y=0l}\Big)\Big(\boldsymbol{E}_{\hat{\boldsymbol{u}}_0}\boldsymbol{W} - \boldsymbol{e}_l \otimes \boldsymbol{g}_{2l} \otimes \boldsymbol{e}_{0M}\Big) \\
&+ \Big(\boldsymbol{E}_l \otimes \boldsymbol{E}_{MM} \otimes \boldsymbol{P}_{xl} \otimes \boldsymbol{\Sigma}_{y=1l}\Big)\Big(\boldsymbol{E}_{\hat{\boldsymbol{u}}_M}\boldsymbol{W} - \boldsymbol{e}_l \otimes \boldsymbol{g}_{3l} \otimes \boldsymbol{e}_{MM}\Big) \\
&+ \Big(\boldsymbol{E}_r \otimes \boldsymbol{E}_{0M} \otimes \boldsymbol{P}_{xr} \otimes \boldsymbol{\Sigma}_{y=0r}\Big)\Big(\boldsymbol{E}_{\hat{\boldsymbol{v}}_0}\boldsymbol{W} - \boldsymbol{e}_r \otimes \boldsymbol{g}_{2r} \otimes \boldsymbol{e}_{0M}\Big) \\
&+ \Big(\boldsymbol{E}_r \otimes \boldsymbol{E}_{MM} \otimes \boldsymbol{P}_{xr} \otimes \boldsymbol{\Sigma}_{y=1r}\Big)\Big(\boldsymbol{E}_{\hat{\boldsymbol{v}}_M}\boldsymbol{W} - \boldsymbol{e}_r \otimes \boldsymbol{g}_{3r} \otimes \boldsymbol{e}_{MM}\Big) \\
&+ \Big(\boldsymbol{E}_r \otimes \boldsymbol{E}_{NrNr} \otimes \boldsymbol{P}_y \otimes \boldsymbol{\Sigma}_{x=1}\Big)\Big(\boldsymbol{E}_{\boldsymbol{v}_{Nr}}\boldsymbol{W} - \boldsymbol{e}_r \otimes \boldsymbol{e}_{NrNr} \otimes \boldsymbol{g}_4\Big)
\end{aligned} \tag{53}$$

$\boldsymbol{E}_{ij}$ in eq.(53) is defined as in eq.(43), $\boldsymbol{E}_{u_i}$ is defined such that the only nonzero elements in $\boldsymbol{E}_{\boldsymbol{u}_i}\boldsymbol{W}$ is the ones corresponding to $\boldsymbol{u}_i$, and

$$\boldsymbol{E}_l = \begin{bmatrix} 1 & 0 \\ 0 & 0 \end{bmatrix}, \quad \boldsymbol{E}_r = \begin{bmatrix} 0 & 0 \\ 0 & 1 \end{bmatrix}, \quad \boldsymbol{e}_l = \begin{bmatrix} 1 \\ 0 \end{bmatrix}, \quad \boldsymbol{e}_r = \begin{bmatrix} 0 \\ 1 \end{bmatrix} \tag{54}$$

$\boldsymbol{\Sigma}_i$ are the penalty matrices at the outer boundaries. $\boldsymbol{\Sigma}_{int}$ is the penalty matrix at the interface between the two regions. Now let a "tilde" sign indicate the $(6M \times 6M)$ (for the sixth order case) block that couples the solutions in the left and right domains.

$$\boldsymbol{\Sigma}_{int} = \begin{bmatrix} 0 & & 0 \\ & \tilde{\boldsymbol{\Sigma}}_{int} & \\ 0 & & 0 \end{bmatrix}, \tag{55}$$

$$\tilde{\boldsymbol{\Sigma}}_{int} = \begin{bmatrix} -\boldsymbol{P}_y \otimes \boldsymbol{\Sigma}_{x=0l} & \boldsymbol{P}_y \otimes \boldsymbol{\Sigma}_{x=0l}\boldsymbol{\Gamma} \\ \boldsymbol{P}_y \otimes \boldsymbol{\Sigma}_{x=0r}\boldsymbol{\Gamma}^{-1} & -\boldsymbol{P}_y \otimes \boldsymbol{\Sigma}_{x=0r} \end{bmatrix}, \tag{56}$$

$$\tilde{\boldsymbol{Q}}_x = \frac{1}{2}\begin{bmatrix} \boldsymbol{P}_y \otimes \boldsymbol{A} & 0 \\ 0 & -\boldsymbol{P}_y \otimes \boldsymbol{A} \end{bmatrix}. \tag{57}$$

Now we can split $\tilde{\boldsymbol{Q}}_x + \tilde{\boldsymbol{\Sigma}}_{int}$ into a symmetric and a skew-symmetric part as

$$\begin{aligned}\tilde{\boldsymbol{Q}}_x + \tilde{\boldsymbol{\Sigma}}_{int} = &\underbrace{\frac{(\tilde{\boldsymbol{Q}}_x + \tilde{\boldsymbol{\Sigma}}_{int}) - (\tilde{\boldsymbol{Q}}_x + \tilde{\boldsymbol{\Sigma}}_{int})^T}{2}}_{\tilde{\boldsymbol{Q}}_x^{sk}} \\ &+ \underbrace{\frac{(\tilde{\boldsymbol{Q}}_x + \tilde{\boldsymbol{\Sigma}}_{int}) + (\tilde{\boldsymbol{Q}}_x + \tilde{\boldsymbol{\Sigma}}_{int})^T}{2}}_{\tilde{\boldsymbol{D}}}\end{aligned} \tag{58}$$

We obtain

$$\tilde{\boldsymbol{Q}}_x^{sk} = \frac{1}{2}\begin{bmatrix} 0 & \boldsymbol{P}_y \otimes \left(\boldsymbol{\Sigma}_{x=0l}\boldsymbol{\Gamma} - \boldsymbol{\Gamma}^{-1}\boldsymbol{\Sigma}_{x=0r}^T\right) \\ \boldsymbol{P}_y \otimes \left(\boldsymbol{\Sigma}_{x=0r}\boldsymbol{\Gamma}^{-1} - \boldsymbol{\Gamma}\boldsymbol{\Sigma}_{x=0l}^T\right) & 0 \end{bmatrix}, \tag{59}$$

$$\tilde{\boldsymbol{D}} = \frac{1}{2}\begin{bmatrix} \boldsymbol{P}_y \otimes \left(\boldsymbol{A} - \boldsymbol{\Sigma}_{x=0l} - \boldsymbol{\Sigma}_{x=0l}^T\right) & \boldsymbol{P}_y \otimes \left(\boldsymbol{\Sigma}_{x=0l}\boldsymbol{\Gamma} + \boldsymbol{\Gamma}^{-1}\boldsymbol{\Sigma}_{x=0r}^T\right) \\ \boldsymbol{P}_y \otimes \left(\boldsymbol{\Gamma}\boldsymbol{\Sigma}_{x=0l}^T + \boldsymbol{\Sigma}_{x=0r}\boldsymbol{\Gamma}^{-1}\right) & \boldsymbol{P}_y \otimes \left(- \boldsymbol{A} - \boldsymbol{\Sigma}_{x=0r} - \boldsymbol{\Sigma}_{x=0r}^T\right) \end{bmatrix}. \tag{60}$$

It was shown in section 4.1 that the method preserves the conservative character if we have $\boldsymbol{\Sigma}_{x=0r} = (\boldsymbol{\Sigma}_{x=0l} - \boldsymbol{A})\boldsymbol{\Gamma}^{-1}$. By introducing this condition, requiring $\boldsymbol{\Sigma}_{x=0l}$ and $\boldsymbol{\Sigma}_{x=0r}$ to be symmetric and add the scaling condition that $\boldsymbol{\Sigma}_{x=0l} = \boldsymbol{\Sigma}_{x=0l}\boldsymbol{\Gamma}$, i.e.

$$\boldsymbol{\Sigma}_{x=0l} = \begin{bmatrix} \lambda_1 & 0 & \frac{1}{2} \\ 0 & 0 & 0 \\ \frac{1}{2} & 0 & \lambda_2 \end{bmatrix} \quad \text{and} \quad \boldsymbol{\Sigma}_{x=0r} = \begin{bmatrix} \lambda_1 & 0 & -\frac{1}{2} \\ 0 & 0 & 0 \\ -\frac{1}{2} & 0 & \lambda_2 \end{bmatrix}, \tag{61}$$

we can factorize $\tilde{\boldsymbol{Q}}_x^{sk}$ and $\tilde{\boldsymbol{D}}$. The final form of the operators becomes

$$\begin{aligned}\tilde{\boldsymbol{Q}}_x^{sk} &= \frac{1}{2}\begin{bmatrix} 0 & 1 \\ -1 & 0 \end{bmatrix} \otimes \boldsymbol{P}_y \otimes \boldsymbol{A}, \\ \tilde{\boldsymbol{D}} &= \frac{1}{2}\begin{bmatrix} 1 & -1 \\ -1 & 1 \end{bmatrix} \otimes \boldsymbol{P}_y \otimes \left(\boldsymbol{A} - 2\boldsymbol{\Sigma}_{x=0l}\right).\end{aligned} \tag{62}$$

To get an energy estimate we multiply eq.(51) with $\boldsymbol{W}^T$ and add its transpose. We obtain

$$\boldsymbol{W}^T\boldsymbol{P}\boldsymbol{W}_t + \boldsymbol{W}_t^T\boldsymbol{P}^T\boldsymbol{W} = \frac{d}{\mathrm{dt}}\|\boldsymbol{W}\|_P^2, \tag{63}$$

$$
\begin{aligned}
-\boldsymbol{W}^T\boldsymbol{Q}_y\boldsymbol{W} - \left(\boldsymbol{W}^T\boldsymbol{Q}_y\boldsymbol{W}\right)^T + \boldsymbol{W}^T\boldsymbol{B}\boldsymbol{C}_{n,s} + \left(\boldsymbol{W}^T\boldsymbol{B}\boldsymbol{C}_{n,s}\right)^T \\
= \hat{\boldsymbol{u}}_0^T\Big(\boldsymbol{P}_{xl}\otimes\left(\boldsymbol{B}+\boldsymbol{\Sigma}_{y=0}+\boldsymbol{\Sigma}_{y=0}^T\right)\Big)\hat{\boldsymbol{u}}_0 \\
+ \hat{\boldsymbol{u}}_M^T\Big(\boldsymbol{P}_{xl}\otimes\left(-\boldsymbol{B}+\boldsymbol{\Sigma}_{y=1}+\boldsymbol{\Sigma}_{y=1}^T\right)\Big)\hat{\boldsymbol{u}}_M \\
+ \hat{\boldsymbol{v}}_0^T\Big(\boldsymbol{P}_{xr}\otimes\left(\boldsymbol{B}+\boldsymbol{\Sigma}_{y=0}+\boldsymbol{\Sigma}_{y=0}^T\right)\Big)\hat{\boldsymbol{v}}_0 \\
+ \hat{\boldsymbol{v}}_M^T\Big(\boldsymbol{P}_{xr}\otimes\left(-\boldsymbol{B}+\boldsymbol{\Sigma}_{y=1}+\boldsymbol{\Sigma}_{y=1}^T\right)\Big)\hat{\boldsymbol{v}}_M \\
- 2\hat{\boldsymbol{u}}_0^T\left(\boldsymbol{P}_{xl}\otimes\boldsymbol{\Sigma}_{y=0}\right)\boldsymbol{g}_{2l} - 2\hat{\boldsymbol{u}}_M^T\left(\boldsymbol{P}_{xl}\otimes\boldsymbol{\Sigma}_{y=1}\right)\boldsymbol{g}_{3l} \\
- 2\hat{\boldsymbol{v}}_0^T\left(\boldsymbol{P}_{xr}\otimes\boldsymbol{\Sigma}_{y=0}\right)\boldsymbol{g}_{2r} - 2\hat{\boldsymbol{v}}_M^T\left(\boldsymbol{P}_{xr}\otimes\boldsymbol{\Sigma}_{y=1}\right)\boldsymbol{g}_{3r},
\end{aligned}
\tag{64}
$$

$$
\begin{aligned}
-\boldsymbol{W}^T\left(\boldsymbol{Q}_x+\boldsymbol{\Sigma}_{int}\right)\boldsymbol{W} - \left(\boldsymbol{W}^T\left(\boldsymbol{Q}_x+\boldsymbol{\Sigma}_{int}\right)\boldsymbol{W}\right)^T \\
+ \boldsymbol{W}^T\boldsymbol{B}\boldsymbol{C}_{e,w} + \left(\boldsymbol{W}^T\boldsymbol{B}\boldsymbol{C}_{e,w}\right)^T \\
= \boldsymbol{u}_0^T\Big(\boldsymbol{P}_y\otimes\left(\boldsymbol{A}+\boldsymbol{\Sigma}_{x=-1}+\boldsymbol{\Sigma}_{x=-1}^T\right)\Big)\boldsymbol{u}_0 \\
+ \boldsymbol{v}_{Nr}^T\Big(\boldsymbol{P}_y\otimes\left(-\boldsymbol{A}+\boldsymbol{\Sigma}_{x=1}+\boldsymbol{\Sigma}_{x=1}^T\right)\Big)\boldsymbol{v}_{Nr} \\
+ 2\boldsymbol{u}_0^T\left(\boldsymbol{P}_y\otimes\boldsymbol{\Sigma}_{x=-1}\right)\boldsymbol{g}_1 - 2\boldsymbol{v}_M^T\left(\boldsymbol{P}_y\otimes\boldsymbol{\Sigma}_{x=1}\right)\boldsymbol{g}_4 \\
- \boldsymbol{W}_{int}^T 2\tilde{\boldsymbol{D}}\boldsymbol{W}_{int},
\end{aligned}
\tag{65}
$$

where $\boldsymbol{W}_{int} = (\boldsymbol{u}_{Nl}, \boldsymbol{v}_0)^T$. We now choose our penalty parameters, at the outer boundary, such that the quadratic terms vanishes, i.e.

$$
\begin{aligned}
\boldsymbol{\Sigma}_{x=-1} = \begin{bmatrix} 0 & 0 & -1 \\ 0 & 0 & 0 \\ 0 & 0 & 0 \end{bmatrix}, \quad \boldsymbol{\Sigma}_{x=1} = \begin{bmatrix} 0 & 0 & 1 \\ 0 & 0 & 0 \\ 0 & 0 & 0 \end{bmatrix} \\
\boldsymbol{\Sigma}_{y=0} = \begin{bmatrix} 0 & 1 & 0 \\ 0 & 0 & 0 \\ 0 & 0 & 0 \end{bmatrix}, \quad \boldsymbol{\Sigma}_{y=1} = \begin{bmatrix} 0 & -1 & 0 \\ 0 & 0 & 0 \\ 0 & 0 & 0 \end{bmatrix}.
\end{aligned}
\tag{66}
$$

If we now summarize, the final version of the energy estimate has the form

$$
\frac{d}{dt}\|\boldsymbol{W}\|_P^2 = \boldsymbol{W}^T\boldsymbol{K}(\boldsymbol{W}+\boldsymbol{G}) = \big(\text{using eq.(66)}\big) = \boldsymbol{B}\boldsymbol{T} + \boldsymbol{I}\boldsymbol{T} \tag{67}
$$

In eq.(67), $\boldsymbol{G}$ includes the boundary values. The structure of $\boldsymbol{K}$ and the $6M \times 6M$, for the sixth order case, matrix $\tilde{\boldsymbol{D}}$, with M=20, Nl=20, Nr=20, can be seen in figure 6.

The boundary and interface terms becomes

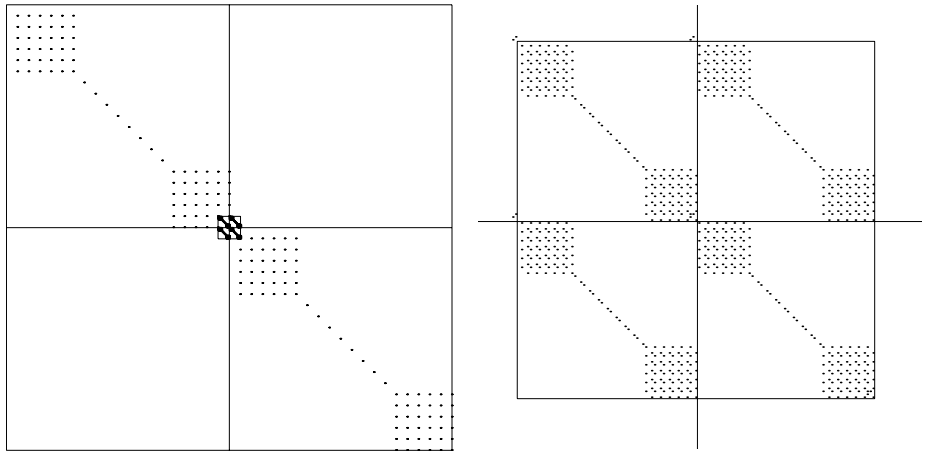

(a) (b)

Figure 6. The structure of the matrix in the energy estimate. (a) the total matrix $\boldsymbol{K}$. (b) the $6M \times 6M$ matrix $\tilde{\boldsymbol{D}}$ in the center of $\boldsymbol{K}$ which couples the two regions.

$$\begin{aligned}\boldsymbol{BT} = &\underbrace{-2\boldsymbol{u}_0^T\Big(\boldsymbol{P}_y \otimes \boldsymbol{\Sigma}_{x=-1}\Big)\boldsymbol{g}_1}_{\boldsymbol{BT}_{west}} \underbrace{-2\boldsymbol{v}_{nr}^T\Big(\boldsymbol{P}_y \otimes \boldsymbol{\Sigma}_{x=1}\Big)\boldsymbol{g}_4}_{\boldsymbol{BT}_{east}} \\ &\underbrace{-2\hat{\boldsymbol{u}}_0^T\Big(\boldsymbol{P}_{xl} \otimes \boldsymbol{\Sigma}_{y=0}\Big)\boldsymbol{g}_{2l} - 2\hat{\boldsymbol{v}}_0^T\Big(\boldsymbol{P}_{xr} \otimes \boldsymbol{\Sigma}_{y=0}\Big)\boldsymbol{g}_{2r}}_{\boldsymbol{BT}_{south}} \\ &\underbrace{-2\hat{\boldsymbol{u}}_M^T\Big(\boldsymbol{P}_{xl} \otimes \boldsymbol{\Sigma}_{y=1}\Big)\boldsymbol{g}_{3l} - 2\hat{\boldsymbol{v}}_M^T\Big(\boldsymbol{P}_{xr} \otimes \boldsymbol{\Sigma}_{y=1}\Big)\boldsymbol{g}_{3r}}_{\boldsymbol{BT}_{north}}\end{aligned} \tag{68}$$

and

$$\boldsymbol{IT} = -2\boldsymbol{W}_{int}^T\tilde{\boldsymbol{D}}\boldsymbol{W}_{int} \tag{69}$$

respectively. Note the similarity between eq.(35) and eq.(68). To get a stable method we must make sure that $\tilde{\boldsymbol{D}}$ is positive semidefinite. We achieve this by choosing $\lambda_1, \lambda_2 \leq 0$ in eq.(61). Note: we can obtain a strictly stable method by setting the ingoing characteristic variables at the outer boundaries.

5 Numerical experiments

To evaluate the method we consider a plane wave which propagates over the discontinuity. The outer boundary data are given by the analytic solution. For the time integration we use the classical fourth order Runge-Kutta method.

5.1 The divergence

Figure 7 show the numerical divergence and L_2 error as a function of time for different orders of accuracy. If the initial data is approximately divergence free, the divergence error will not dominate over the computational error. The fact that we do not explicitly satisfy eq.(1) does not seem to introduce any significant error. In the high order accuracy case, the divergence will stay well below the computational error.

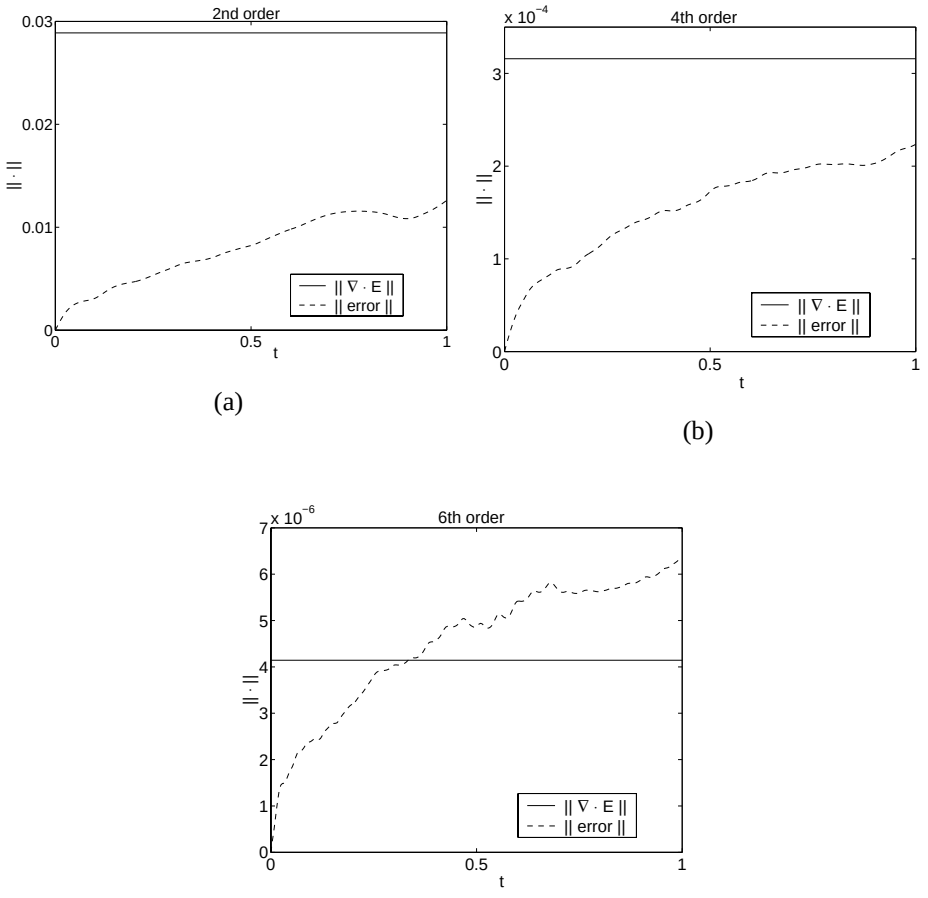

Figure 7. Plot of $||\nabla \cdot \boldsymbol{E}||_2$ and $||error||_2$. (a) 2nd order accuracy, (b) 4th order accuracy, (c) 6th order accuracy. M=40, Nl=40, Nr=40

Consider eq.(4) in the semi discrete case. The fact that our SBP operators satisfy the property $\boldsymbol{D}_x\boldsymbol{D}_y = \boldsymbol{D}_y\boldsymbol{D}_x$ leads to

$$\nabla_d \cdot \frac{\partial}{\partial t}\boldsymbol{E} + \nabla_d \cdot \boldsymbol{J} = \nabla_d \cdot \nabla_d \times \boldsymbol{H} = 0. \tag{70}$$

We will have the same result in the semi discrete case as in the continuous case, i.e.

$$\left(\nabla_d \cdot \boldsymbol{E} - \frac{\rho}{\epsilon}\right)(t) = \left(\nabla_d \cdot \boldsymbol{E} - \frac{\rho}{\epsilon}\right)(0). \tag{71}$$

In the computations the analytic solution is used as initial data and $\rho = 0$. Away from the interface, we have $\nabla_d \cdot \boldsymbol{E}(0) = \nabla \cdot \hat{\boldsymbol{E}}(0) + \mathcal{O}(\Delta x)^p$. Here $\hat{\boldsymbol{E}}$ is the exact solution projected on the grid. This means that $\nabla_d \cdot \boldsymbol{E} = \mathcal{O}(\Delta x)^p$ initially, and thus $\nabla_d \cdot \boldsymbol{E} = \mathcal{O}(\Delta x)^p$ for all t. In the 2D case, only the z component of $\boldsymbol{H}$ is present and it is trivial that $\nabla \cdot \boldsymbol{H} = 0$.

We can not compute the divergence at the interface between the two media since we have a discontinuity in the x component of $\boldsymbol{E}$. Therefore we compute the divergence to the left of the interface. Figure 7 show that the divergence of $\boldsymbol{E}$ is constant in time. As mentioned above, the analytic solution at $t = 0$ is divergence free. Hence the divergence shown in the figure is introduced by the numerical computation of $\nabla \cdot \boldsymbol{E}$. In figure 8, we see the long time behavior of the computational error.

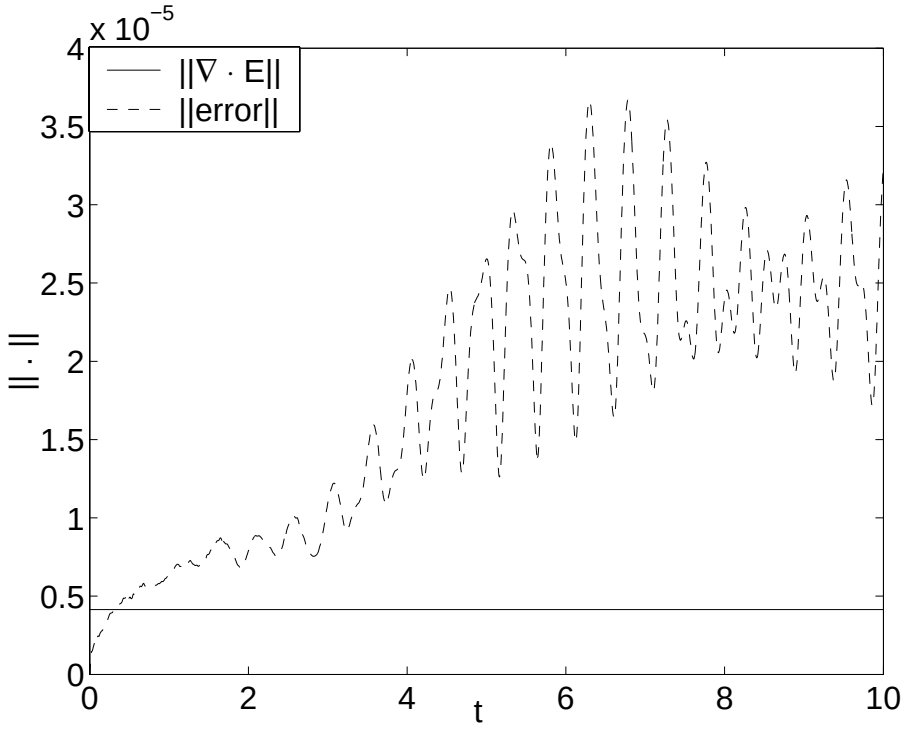

Figure 8. Plot of $||\nabla \cdot \boldsymbol{E}||_2$ and $||error||_2$. 6th order accuracy. M=40, Nl=40, Nr=40

5.2 The order of accuracy

The order of accuracy in space, will be computed by mesh refinement in space for a given time. The solutions are computed with a very small time step.

Stability requirements prohibits the use of the same technique to verify the accuracy in time. In this case we use a technique which eliminates the exact solution and the error imposed by the spatial integration. We have

$$\boldsymbol{u}^{\Delta t,\Delta x} = \hat{\boldsymbol{u}} + \boldsymbol{e}(\Delta t) + \boldsymbol{e}(\Delta x). \tag{72}$$

Where $\boldsymbol{u}^{\Delta t,\Delta x}$ is the numerical solution with step size Δt and Δx in time and space respectively. $\hat{\boldsymbol{u}}$ is the exact solution, $\boldsymbol{e}(\Delta t)$ and $\boldsymbol{e}(\Delta x)$ are the time and space errors respectively. With accuracy of order q in time and of order p in space we have

$$\boldsymbol{e}(\Delta t) = \mathcal{O}(\Delta t)^q, \quad \boldsymbol{e}(\Delta x) = \mathcal{O}(\Delta x)^p. \tag{73}$$

To separate the error imposed by the time integration we use a fixed Δx and compute

$$\frac{\|\boldsymbol{u}^{\Delta t,\Delta x} - \boldsymbol{u}^{\frac{\Delta t}{2},\Delta x}\|}{\|\boldsymbol{u}^{\frac{\Delta t}{2},\Delta x} - \boldsymbol{u}^{\frac{\Delta t}{4},\Delta x}\|} = \frac{\mathcal{O}(\Delta t^q) - \mathcal{O}(\frac{\Delta t}{2})^q}{\mathcal{O}(\frac{\Delta t}{2})^q - \mathcal{O}(\frac{\Delta t}{4})^q} = 2^q. \tag{74}$$

No reflection at the interface

In the first case the wave hits the discontinuity with an angle of incidence that prohibits a reflecting wave. This special angle is known as the *Brewster angle* or *angle of polarization*, Θ_p and is the result of *Brewster's law* [6]

$$\tan\Theta_p = \frac{n_2}{n_1}. \tag{75}$$

n_1 and n_2 are the refraction index of respective medium. The wave is depicted in fig.(9). The accuracy in space is given by figure 10.

Figure 9. The wave in the domain, for $\Theta_i = \Theta_p$. (a) the wave propagating to the left, (b) the wave propagating to the right, (c) the total wave

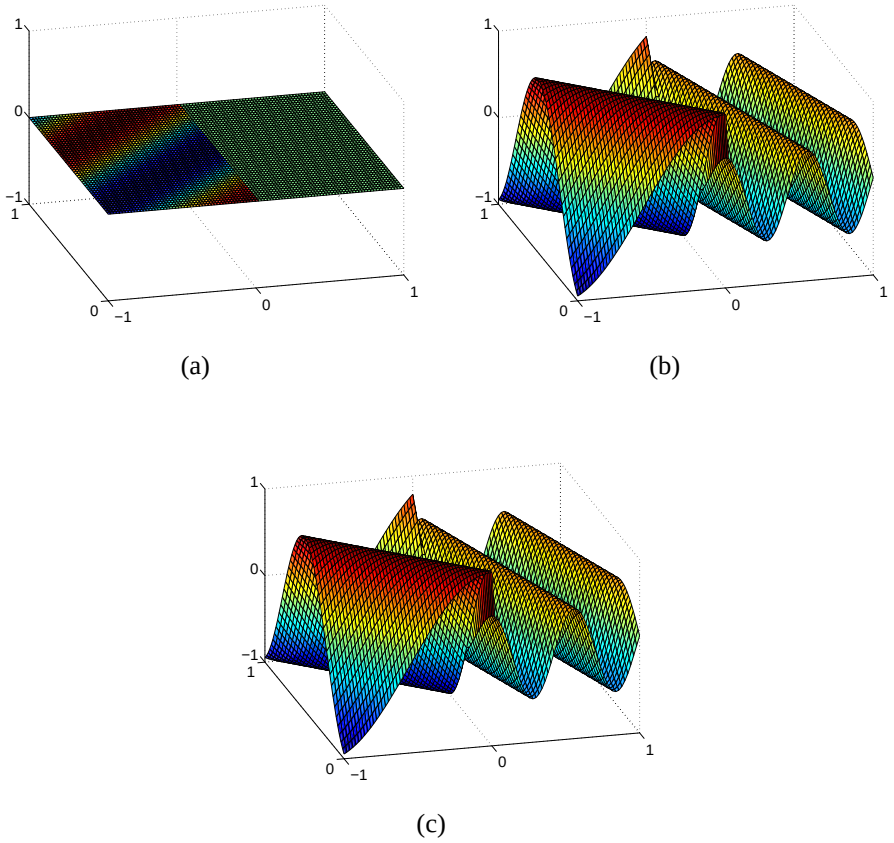

Figure 10. Error at t=1 for varying Δx, with $\Theta_i = \Theta_p$

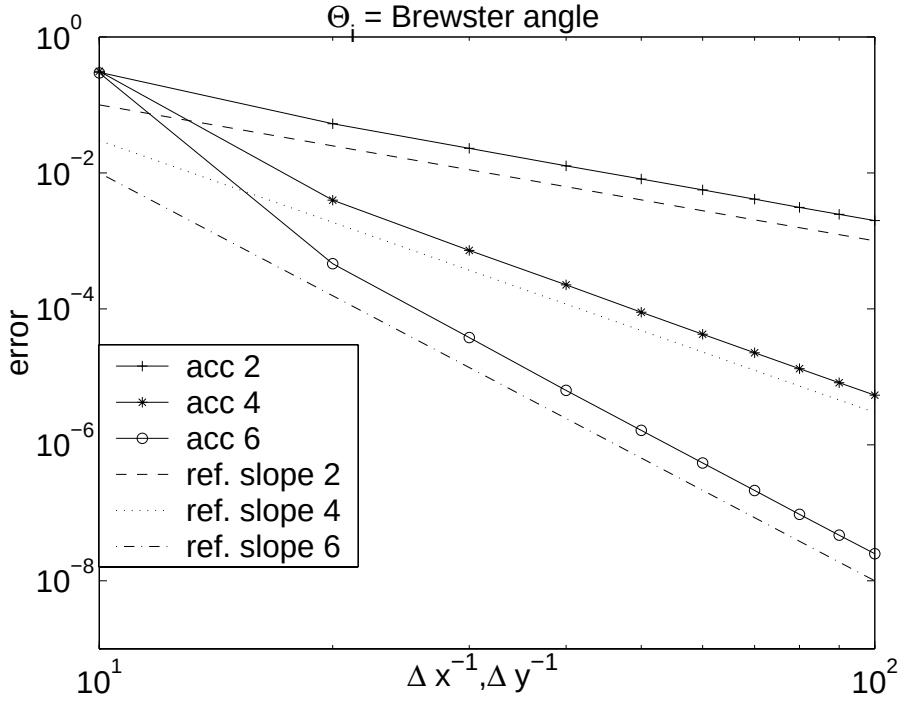

Small reflection at the interface

In this case we use the angle, $\Theta_i = \frac{\pi}{3}$, to accomplish a small reflection at the boundary between the two regions, see figure 11. The accuracy in space is given by fig.(12).

Figure 11. The wave in the domain, for $\Theta_i = \frac{\pi}{3}$. (a) the wave propagating to the left, (b) the wave propagating to the right, (c) the total wave

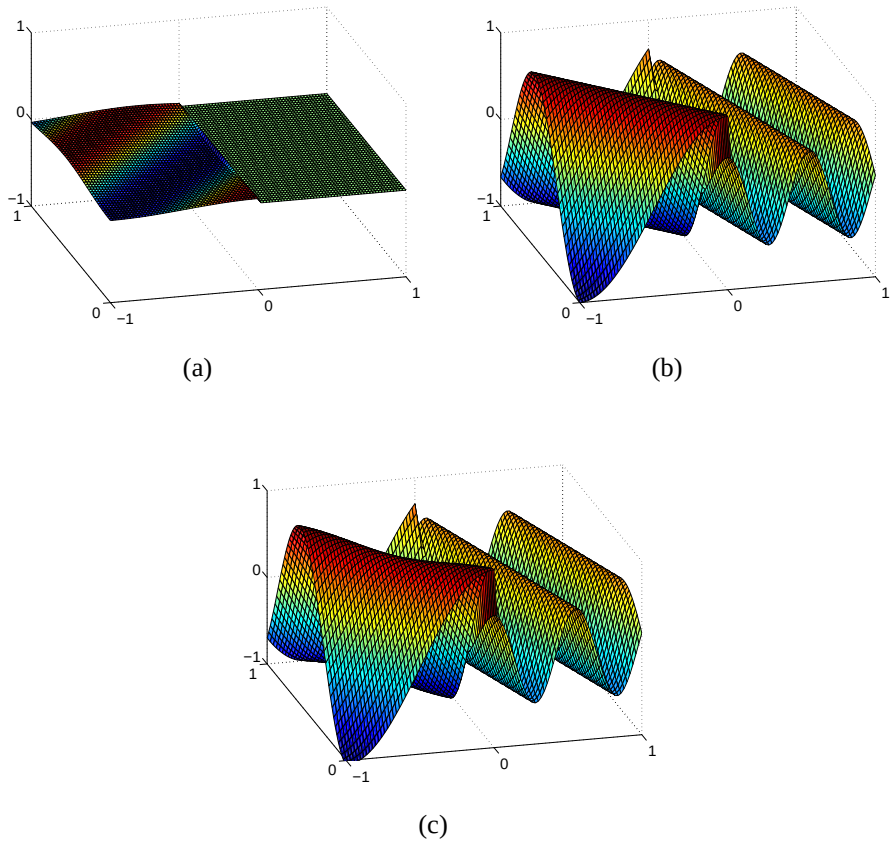

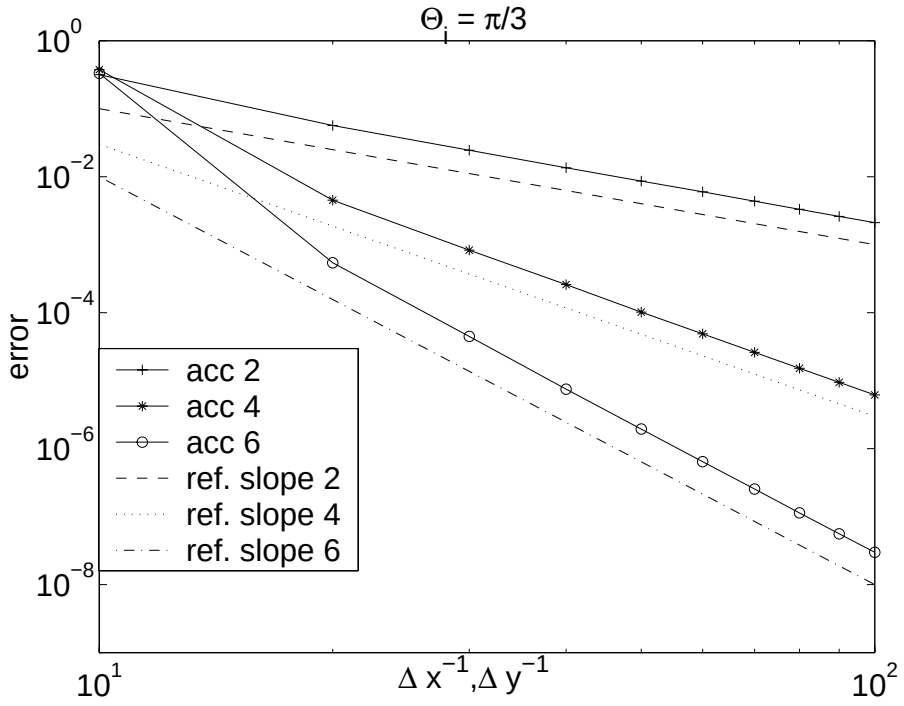

Figure 12. Error at t=1 for varying Δx, with $\Theta_i = \frac{\pi}{3}$

Significant reflection at the interface

The angle $\Theta_i = \frac{\pi}{6}$, will accomplish a significant reflection at the interface between the two medium, see figure 13. The accuracy in space is fulfilled according to fig.(14).

Figure 13. The wave in the domain, for $\Theta_i = \frac{\pi}{6}$. (a) the wave propagating to the left, (b) the wave propagating to the right, (c) the total wave.

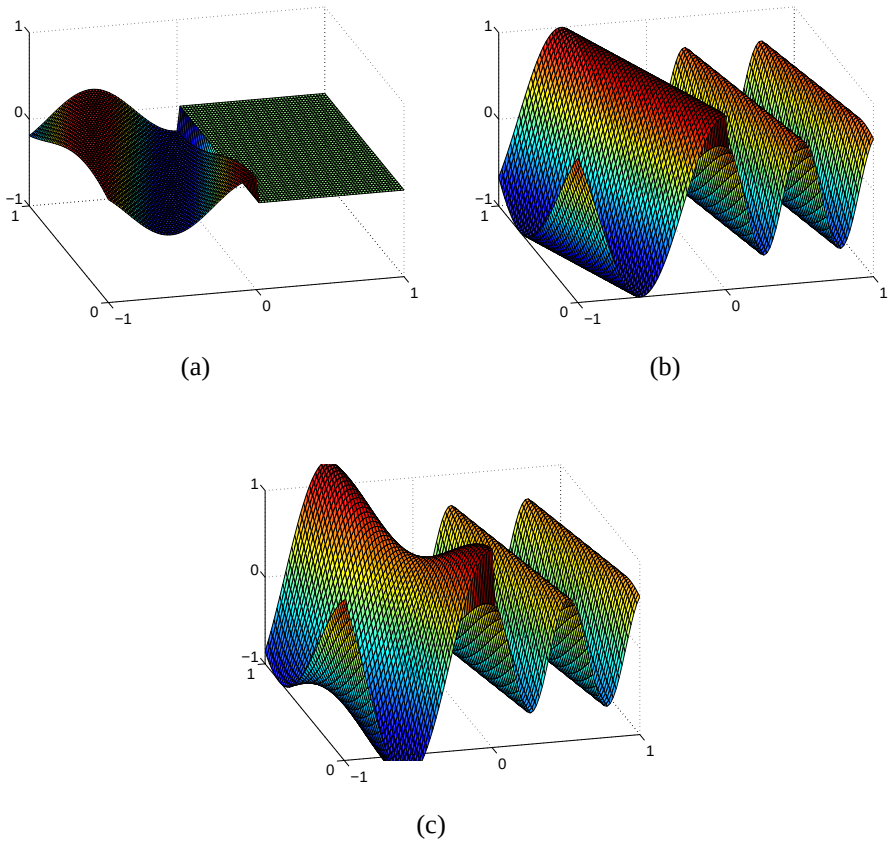

Figure 14. Error at t=1 for varying Δx, with $\Theta_i = \frac{\pi}{6}$.

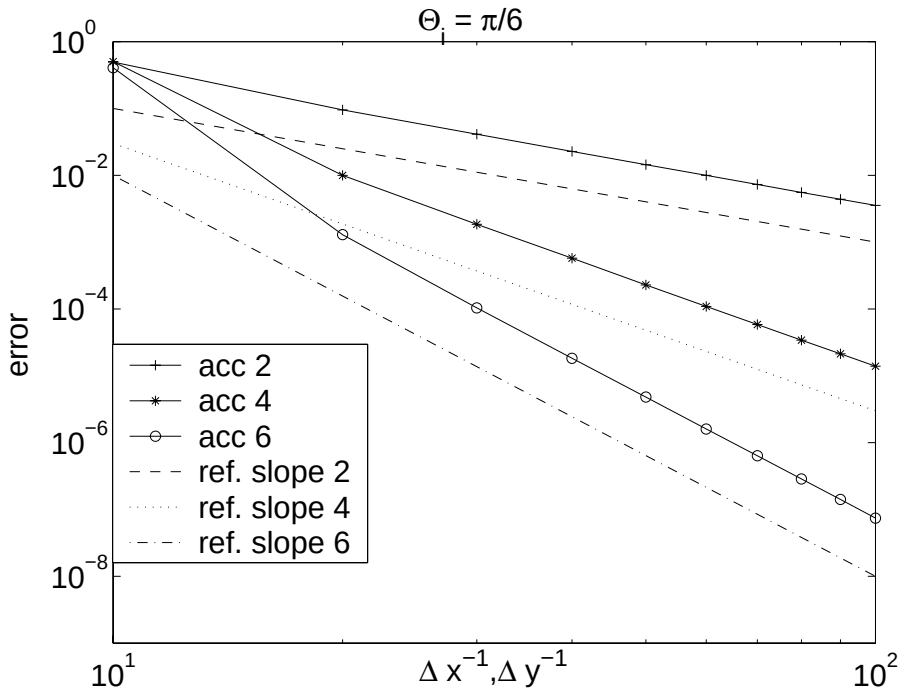

Accuracy in time

The accuracy in time is obtained by evaluation of eq.(74). The result is fourth order accuracy in time as shown in table 1.

Table 1. Result of evaluation of eq.(74) for different Θ_i

Θ_i	Evaluation of eq.(74)
Θ_p	$16.9 \approx 2^4$
$\frac{\pi}{3}$	$17.4 \approx 2^4$
$\frac{\pi}{6}$	$16.5 \approx 2^4$

5.3 The spectrum

To analyze the numerical stability we consider the matrix $\boldsymbol{A} - 2\boldsymbol{\Sigma}_{x=0l}$ in eq(62) and the spectrum of the matrix $\boldsymbol{M}$ in eq.(46). Note that a positive semi definite $\tilde{\boldsymbol{D}}$ or

$$\boldsymbol{A} - 2\boldsymbol{\Sigma}_{x=0l} = \begin{bmatrix} -2\lambda_1 & 0 & 0 \\ 0 & 0 & 0 \\ 0 & 0 & -2\lambda_2 \end{bmatrix}, \quad \lambda_1, \lambda_2 \leq 0, \tag{76}$$

is required for stability. The spectrum depends on the penalty parameters in $\boldsymbol{\Sigma}_{x=0l}$, $\boldsymbol{\Sigma}_{x=0r}$ and is depicted in figure 15 - 18.

The parameter values $\lambda_1 = 0, \lambda_2 = 0$ leads to $\tilde{\boldsymbol{D}} = 0$ which means that we have zero dissipation. The spectrum is shown in figure 15.

Figure 15. Spectrum for matrix $\boldsymbol{M}$ in eq.(46) for $\lambda_1 = 0, \lambda_2 = 0$.

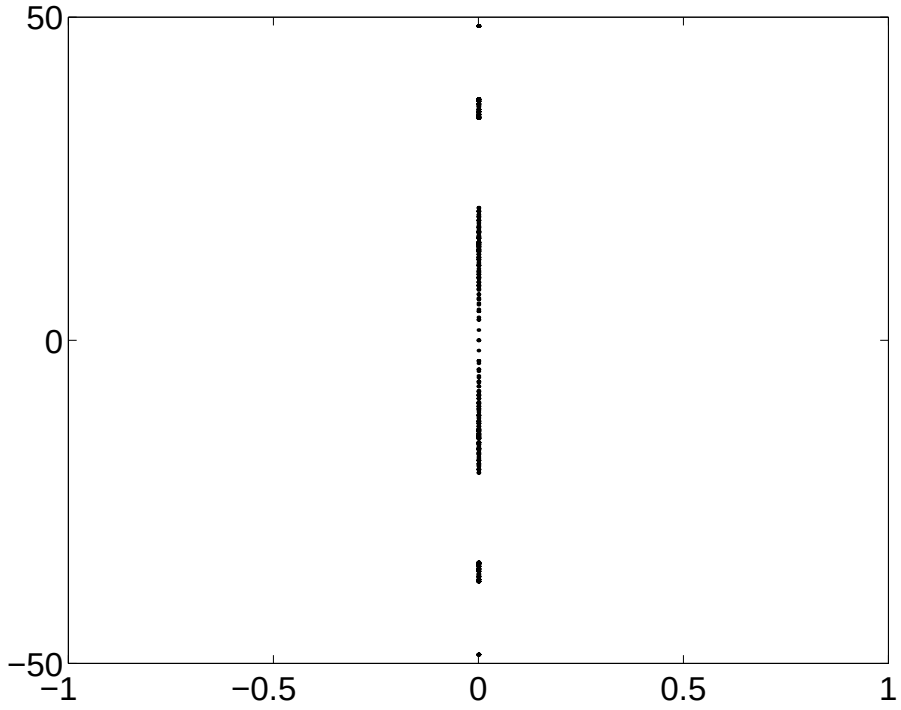

The parameter values $\lambda_1 = -0.1, \lambda_2 = -0.1$ introduces dissipation as can be seen in eq.(76) and figure 16

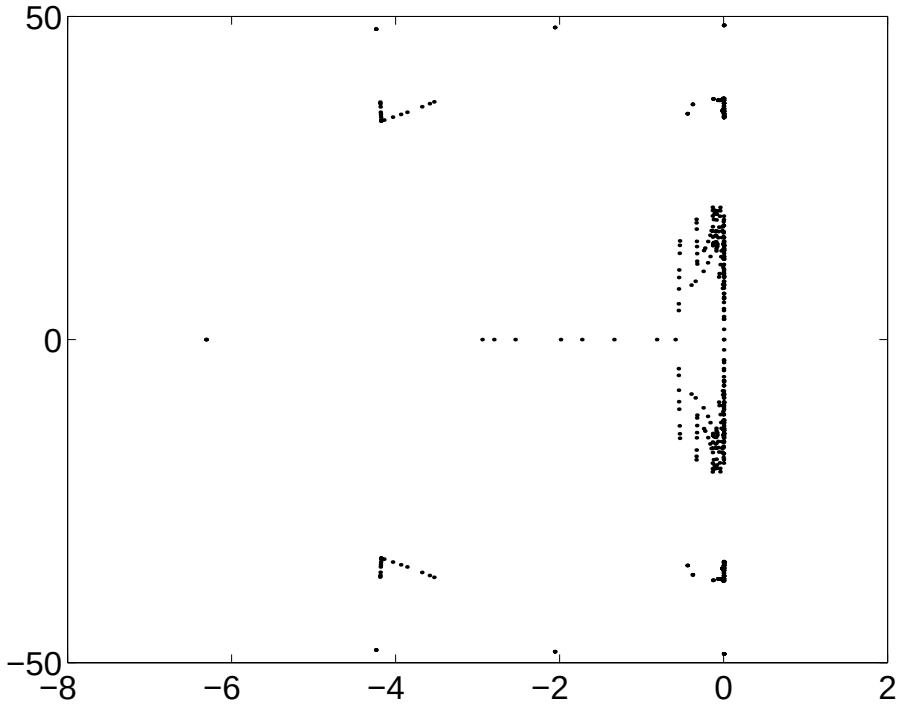

Figure 16. Spectrum for matrix $\boldsymbol{M}$ in eq.(46) for $\lambda_1 = -0.1, \lambda_2 = -0.1$.

The increasing amount of dissipation corresponds to a shift in the spectrum towards the negative real axis, see figures 17 - 18.

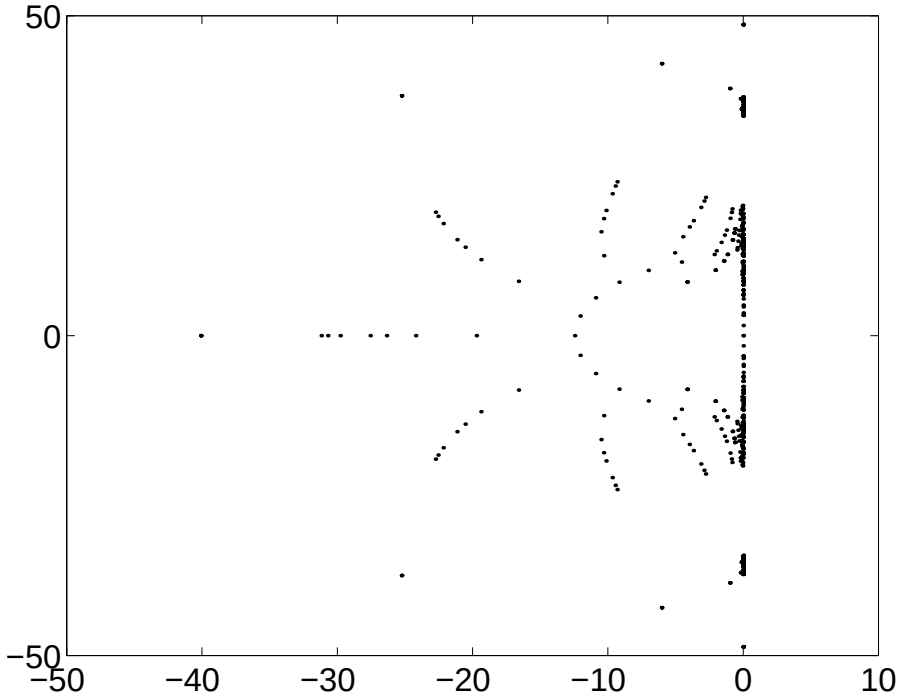

Figure 17. Spectrum for matrix $\boldsymbol{M}$ in eq.(46) for $\lambda_1 = -0.5, \lambda_2 = -0.5$.

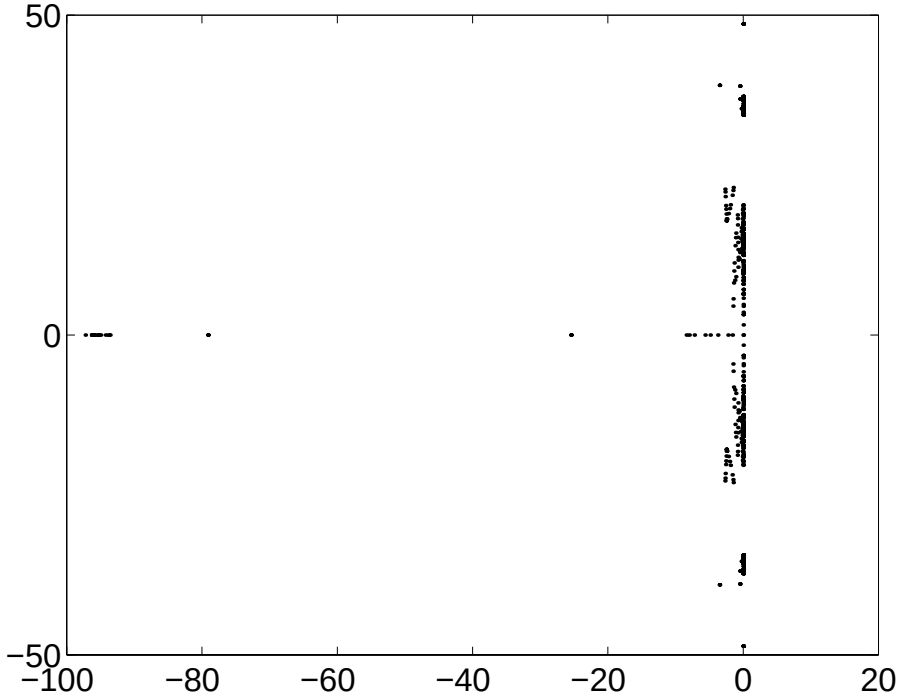

Figure 18. Spectrum for matrix $\boldsymbol{M}$ in eq.(46) for $\lambda_1 = -1.0, \lambda_2 = -1.0$.

6 Conclusions

Wave propagation close to a material discontinuity have been simulated. The physical interface conditions for the electromagnetic field have been derived. To simulate the electromagnetic wave we have used SBP operators of second, fourth and sixth order accuracy. The boundary conditions have been imposed by the SAT procedure. We have shown that we can control the stability by the choice of penalty parameters in the SAT procedure.

The simulations was made for several angles of incidence to the material interface between the two media. For each case we have verified the order of accuracy in space and time. The divergence has been shown to be constant in time for uniform meshes. A material discontinuity will cause no problem when simulating an electromagnetic wave using SBP operators.

Appendix A

The Kronecker product

Definition 1 *Let $\boldsymbol{A}$ be a $p \times q$ matrix and let $\boldsymbol{B}$ be an $m \times n$ matrix, then*

$$\boldsymbol{A} \otimes \boldsymbol{B} = \begin{pmatrix} a_{0,0}\boldsymbol{B} & \cdots & a_{0,q-1}\boldsymbol{B} \\ \vdots & \ddots & \vdots \\ a_{p-1,0}\boldsymbol{B} & \cdots & a_{P-1,0}\boldsymbol{B} \end{pmatrix} \tag{77}$$

The $p \times q$ block matrix $\boldsymbol{A} \otimes \boldsymbol{B}$ is called a Kronecker product.

There are a number of rules for Kronecker products, see [3], we will present some of them. Let $\boldsymbol{A}$, $\boldsymbol{B}$, $\boldsymbol{C}$ and $\boldsymbol{D}$ be matrices of arbitrary sizes, such that the specified operations are defined.

$$\begin{aligned} (\boldsymbol{A} \otimes \boldsymbol{B})(\boldsymbol{C} \otimes \boldsymbol{D}) &= (\boldsymbol{A}\boldsymbol{C}) \otimes (\boldsymbol{B}\boldsymbol{D}) \\ (\boldsymbol{A} + \boldsymbol{B}) \otimes \boldsymbol{C} &= \boldsymbol{A} \otimes \boldsymbol{C} + \boldsymbol{B} \otimes \boldsymbol{C} \\ (\boldsymbol{A} \otimes \boldsymbol{B})^T &= \boldsymbol{A}^T \otimes \boldsymbol{B}^T \\ (\boldsymbol{A} \otimes \boldsymbol{B})^{-1} &= \boldsymbol{A}^{-1} \otimes \boldsymbol{B}^{-1} \\ \boldsymbol{A} > 0 \quad , \quad \boldsymbol{B} > 0 &\Rightarrow (\boldsymbol{A} \otimes \boldsymbol{B}) > 0 \end{aligned} \tag{78}$$

References

[1] H. O. Kreiss B. Gustafsson and J. Oliger. *Time Dependent Problems and Difference Methods*. John Wiley & Sons, Inc, 1995.

[2] H. O. Kreiss and G Scherer. Finite element and einite difference methods for hyperbolic partial differential equations. in mathematical aspects of finite elements in differential equations. *Academic Press, New York*, 1974.

[3] C. Van Loan. Computational frameworks for the fast fourier transform. *SIAM*, 1992.

[4] D. Gottlieb M. H. Carpenter and S. Abarbanel. *Journal of Computational Physics, 111:220-236*, 1994.

[5] J. Nordström and M. H. Carpenter. High order finite difference methods, multidimensional linear problems and curvilinear coordinates. *ICASE Report*, (99-54), 2000.

[6] R. K. Wangsness. *Electromagnetic Fields*. John Wiley & Sons, Inc, second edition, 1986.

Issuing organisation
FOI – Swedish Defence Research Agency
Division of Aeronautics, FFA
SE-172 90 STOCKHOLM

Report number, ISRN
FOI-R–0120–SE

Report type
Scientific Report

Month year
April 2001

Project number
E840243

Customers code
3. Aeronautical Research

Research area code
6. Electric Warfare

Sub area code
62. Stealth Technology

Author(s)
Rikard Gustafsson and Jan Nordström

Project manager
Jan Nordström

Approved by
Torsten Berglind
Head, Computational Aerodynamics Department

Scientifically and technically responsible
Jan Nordström

Report title
High Order Finite Difference Approximations of Electromagnetic Wave Propagation Close to Material Discontinuities

Abstract
In this paper, electromagnetic wave propagation close to a material discontinuity has been simulated. We have used summation by part (SBP) operators of second, fourth and sixth order accuracy. The boundary conditions have been imposed by the simultaneous approximation term (SAT) procedure. Stability has been shown and the order of accuracy has been verified numerically.

Keywords
Finite difference, interface condition, stability, electromagnetic wave, material discontinuity

Further bibliographic information

ISSN
ISSN 1650-1942

Pages
47

Language
English

Price
Acc. to price list

Security classification
Unclassified

Utgivare	Rapportnummer, ISRN	Klassificering
Totalförsvarets Forskningsinstitut – FOI Avdelningen för Flygteknik, FFA SE-172 90 STOCKHOLM	FOI-R–0120–SE	Vetenskaplig rapport
	Månad år April 2001	Projektnummer E840243
	Verksamhetsgren 3. Flygteknisk forskning	
	Forskningsområde 6. Telekrig	
	Delområde 62. Signaturanpassning	
Författare Rikard Gustafsson och Jan Nordström	Projektledare Jan Nordström	
	Godkänd av Torsten Berglind Chef, Institutionen för Beräkningsaerodynamik	
	Tekniskt och/eller vetenskapligt ansvarig Jan Nordström	

Rapporttitel

Högre ordningens finit differensapproximation av elektromagnetisk våg nära materialdiskontinuitet

Sammanfattning

I den här rapporten har vi simulerat en elektromagnetisk våg nära en materialdiskontinuitet. Vi har använt oss av ”summation by parts” (SBP)-operatorer av noggrannhetsordning två, fyra och sex. Randdata införs med hjälp av ”simultaneous approximation term” (SAT)-metoden. Vi har visat stabilitet och noggrannhetsordningen har verifierats numeriskt.

Nyckelord

Finita differenser, stabilitet, elektromagnetik, vågutbredning, materialdiskontinuitet

Övriga bibliografiska uppgifter

Examensarbete

ISSN	Antal sidor	Språk
ISSN 1650-1942	47	Engelska
Distribution enligt missiv	Pris Enligt prislista	
	Sekretess Öppen	